

Proteomic Analysis of Dhh1 Complexes Reveals a Role for Hsp40 Chaperone Ydj1 in Yeast P-Body Assembly

Gregory A. Cary,^{*,†,1,2} Dani B. N. Vinh,^{*,1,3} Patrick May,^{*,‡} Rolf Kuestner,^{*,4} and Aimée M. Dudley^{†,§,5}

^{*}Institute for Systems Biology, Seattle, Washington 98109, [†]Molecular and Cellular Biology Program, University of Washington, Seattle, Washington 98195, [‡]Luxembourg Centre for Systems Biomedicine, Université du Luxembourg, Esch-sur-Alzette, Luxembourg L-4362, and [§]Pacific Northwest Diabetes Research Institute, Seattle, Washington 98122
ORCID IDs: 0000-0003-3573-5229 (G.A.C.); 0000-0002-4139-6860 (D.N.V.); 0000-0003-3644-0625 (A.M.D.)

ABSTRACT P-bodies (PB) are ribonucleoprotein (RNP) complexes that aggregate into cytoplasmic foci when cells are exposed to stress. Although the conserved mRNA decay and translational repression machineries are known components of PB, how and why cells assemble RNP complexes into large foci remain unclear. Using mass spectrometry to analyze proteins immunoprecipitated with the core PB protein Dhh1, we show that a considerable number of proteins contain low-complexity sequences, similar to proteins highly represented in mammalian RNP granules. We also show that the Hsp40 chaperone Ydj1, which contains a low-complexity domain and controls prion protein aggregation, is required for the formation of Dhh1–GFP foci on glucose depletion. New classes of proteins that reproducibly coenrich with Dhh1–GFP during PB induction include proteins involved in nucleotide or amino acid metabolism, glycolysis, transfer RNA aminoacylation, and protein folding. Many of these proteins have been shown to form foci in response to other stresses. Finally, analysis of RNA associated with Dhh1–GFP shows enrichment of mRNA encoding the PB protein Pat1 and catalytic RNAs along with their associated mitochondrial RNA-binding proteins. Thus, global characterization of PB composition has uncovered proteins important for PB assembly and evidence suggesting an active role for RNA in PB function.

KEYWORDS

P-bodies
chaperones
microarrays
proteomics

Processing bodies (P-bodies, or PB) and stress granules (SG) are eukaryotically conserved ribonucleoprotein (RNP) granules consisting

of nontranslating mRNA and associated proteins (Eulalio *et al.* 2007a; Kedersha and Anderson 2009; Decker and Parker 2012). PB and SG both accumulate in cytoplasmic foci within minutes of exposure to a variety of environmental stresses (Bregues *et al.* 2005; Teixeira *et al.* 2005; Garmendia-Torres *et al.* 2014), and the appearance of these foci is correlated with global translational arrest common to the early phase of many cellular stress responses (Holcik and Sonenberg 2005; Kedersha and Anderson 2009; Simpson and Ashe 2012). The kinetics of assembly and exact composition of these granules can vary in a stress-specific manner (Buchan *et al.* 2011). PB and SG primarily are distinguished on the basis of their constituent proteins; PB core proteins are associated with mRNA decay functions (Sheth and Parker 2003; Buchan *et al.* 2010), whereas SG consist of translation initiation factors as well as other mRNA-binding proteins (Hoyle *et al.* 2007; Buchan *et al.* 2008; Lui *et al.* 2010; Decker and Parker 2012; Kedersha *et al.* 2013). These granules have been observed to interact *in vivo*, and messenger ribonucleoprotein (mRNP) subcomplexes can exchange between foci (Kedersha *et al.* 2005; Stoecklin and Kedersha 2013). Furthermore, specific proteins can cycle into foci from the cytoplasm in less than a minute

Copyright © 2015 Cary *et al.*

doi: 10.1534/g3.115.021444

Manuscript received August 20, 2015; accepted for publication September 16, 2015; published Early Online September 21, 2015.

This is an open-access article distributed under the terms of the Creative Commons Attribution 4.0 International License (<http://creativecommons.org/licenses/by/4.0/>), which permits unrestricted use, distribution, and reproduction in any medium, provided the original work is properly cited.

Supporting information is available online at www.g3journal.org/lookup/suppl/doi:10.1534/g3.115.021444/-/DC1

Microarray design information and data have been deposited with the Gene Expression Omnibus (GEO) database at National Center for Biotechnology Information under accession no. GSE65989.

¹These authors contributed equally to this work.

²Present address: Department of Biological Sciences, Carnegie Mellon University, Pittsburgh, PA 15216.

³Present address: Department of Biochemistry, University of Washington, Seattle, WA 98195.

⁴Present address: Matrix Genetics, Inc., Seattle, WA 98102.

⁵Corresponding author: Pacific Northwest Diabetes Research Institute, 720 Broadway, Seattle, WA 98122. E-mail: aimée.dudley@gmail.com

(Aizer *et al.* 2008). These observations highlight the dynamic nature of RNP granule assemblies.

Regions of low-complexity (LC) sequence are common among proteins that localize to mammalian RNP granules (Kato *et al.* 2012). LC regions are necessary for both RNP aggregation into cytoplasmic foci (Kato *et al.* 2012) and retention of RNA (Han *et al.* 2012). Recent studies also have shown the prevalence of LC-domains in proteins that affect SG assembly in yeast (Yang *et al.* 2014). Similar Q/N-rich prion-like domains, a specific subset of LC domains, are found in several yeast PB and SG proteins (*e.g.*, Lsm4, Edc3, and Pbp1) and are required for RNP granule aggregation (Gilks *et al.* 2004; Decker *et al.* 2007; Buchan and Parker 2009). Aberrant forms of these RNP granule proteins, with the propensity to form cytotoxic, prion-like aggregates, have been associated with a number of neurodegenerative diseases (Li *et al.* 2013; Ramaswami *et al.* 2013). Although aggregation via LC sequences is a common feature for many RNP proteins, it is the result of a controlled physiological process as opposed to nonspecific protein–protein aggregation. For example, although salt stress induces PB aggregation in wild-type yeast, deletion of the gene encoding the effector kinase for the osmotic shock signal transduction pathway prevents the accumulation of PB foci in the presence of high salt (Teixeira *et al.* 2005).

To date, the functional relevance of RNP granule aggregation remains unclear. The fact that mutant strains that are unable to form foci show a decrease in cell viability (Lavut and Raveh 2012) and long-term survival (Ramachandran *et al.* 2011) suggests that PB/SG aggregation has some important cellular function. Furthermore, PB foci can be transmitted from mother to daughter cells during yeast mitosis, and this transmission provides a measurable growth advantage to the recipient cells (Garmendia-Torres *et al.* 2014). Despite the fact that PB consist of proteins involved in mRNA decay, mRNA decay processes are not affected by perturbations that block the formation of visible PB foci (Decker *et al.* 2007; Eulalio *et al.* 2007b). Thus, an inventory of the proteins and RNA transcripts that localize to these granules and a better understanding of how their composition changes in response to stress induction could shed light on the nature of the cellular benefit of PB/SG aggregation.

Much of our current understanding of the composition and assembly dynamics of PB and SG is based on cytological and genetic experiments that have characterized protein localization to cytoplasmic foci under stress conditions. Previous biochemical studies have identified few core proteins when PB components are purified under native conditions (Fenger-Gron *et al.* 2005; Drummond *et al.* 2011; Bahassou-Benamri *et al.* 2013), likely due to the dynamic nature of RNP granules. Other approaches to characterize PB components have relied on cross-linking and denaturing conditions to capture proteins and associated RNA (Mitchell *et al.* 2013). To better understand both the protein and RNA constituents of PB aggregation during stress induction, we enriched native PB complexes from yeast cells by using an anti-green fluorescent protein (GFP) antibody to isolate a GFP fusion to the core PB component Dhh1. To characterize the components that differentially associate with a putative PB core complex during stress and nonstress conditions, we isolated the Dhh1–GFP complex from cells grown in 2% glucose and acute 0% glucose conditions and used quantitative tandem mass spectrometry (MS) and microarray analyses to identify the proteins and RNAs within the Dhh1 complex. Our results give evidence for PB association of many proteins previously implicated by genetic and cytological studies, and provide a new approach for analyzing the composition and function of these structures upon stress induction.

MATERIALS AND METHODS

Yeast strains and growth conditions

All yeast strains used in this study (Supporting Information, Table S1) are derived from BY4741 (Winston *et al.* 1995). GFP-tagged strains (Huh *et al.* 2003) were purchased from Life Technologies. Individual gene deletions marked by *kanMX* were created by homologous recombination in strains harboring GFP-tagged genes (*e.g.*, *DHH1-GFP*, YAD49). MoBY plasmids are from a library collection of centromere-containing plasmids that contain individual bar-coded yeast open reading frames (ORFs) expressed from their own promoter (Ho *et al.* 2009) that was purchased from ThermoScientific. MoBY plasmids were transformed into YAD557 and tested for Dhh1–GFP foci formation. All genetic manipulations of yeast and growth media are as in standard protocols (Rose *et al.* 1990). Unless otherwise noted, yeast cells were grown in rich media (YPD) at 30°.

For glucose depletion (–glucose) experiments, overnight 5-mL cultures in YPD were serially expanded into a final 2-L culture and grown to late log phase ($OD_{600} = 1.0$). Cells were harvested rapidly by filtration (0.65 μ m pore size; Millipore Nitrocellulose Membrane), and resuspended into fresh 2 L –glucose media (YEP), and the culture was shaken for an additional 30 min. Final cell pellets were collected by filtration, concentrated into conical tubes by low speed (500g) centrifugation, and flash-frozen in liquid nitrogen.

A stable isotope labeling by amino acids in cell culture (SILAC) culture of wild-type cells was generated using a modified I-DIRT (Tackett *et al.* 2005) protocol. To summarize in brief, BY4741 was first grown to a late log density of $OD_{600} = 1$ in synthetic complete media lacking lysine and arginine (SC–lys–arg), containing 2% glucose and supplemented with 50 mg/L each of lysine and arginine. This culture was then diluted and grown for a total of 9 doublings to $OD_{600} \sim 1.2$ in SC–lys–arg 2% glucose media supplemented with 50 mg/L each of heavy-isotopically labeled arginine ($^{13}C6$ - $^{15}N4$) and lysine ($^{13}C6$ - $^{15}N2$). Cells were filtered and frozen as described previously.

Cell lysis and immunoaffinity purification

Cell pellets stored at –80° were released into a precooled Retsch PM-100 planetary ball mill grinding jar. Grinding was performed at ~ 30 g in 2-min cycles with rotation reversals at 1 min. Jars were rechilled in liquid nitrogen between grinding cycles. Samples were ground until >90% lysis was achieved, which typically occurred after 5–10 cycles of grinding. The cell powder grindate was collected and returned to –80° for storage.

Anti-GFP IgG (catalog no. 11814460001; Roche) coupled to magnetic Protein-G Dynabeads (Invitrogen) was used to capture Dhh1–GFP protein complexes from yeast cell lysate. Anti-GFP was first crosslinked to protein-G bead in 20 mM dimethyl pimelimidate (Thermo Scientific) with the use of protocols recommended by the manufacturer. A ratio of 30 mg of Ab-proG beads to 300 mg of total protein captured >90% of Dhh1–GFP in the cell lysate, as determined by Western blot analysis. Cell lysate generated from 4 L of cell culture was used to obtain sufficient material for MS. To generate a lysate supernatant, cell powder grindate was thawed quickly by resuspending in 1.5 volumes of RB buffer [30 mM K-Hepes (pH 7.4), 150 mM KCl, 2 mM $MgCl_2$, 0.2% NP-40, 0.1% Tween-20, 1 mM dithiothreitol, yeast protease inhibitor cocktail (Sigma-Aldrich), and RNase-inhibitor (Ambion / Millipore)]. The suspension was subsequently cleared by low-speed centrifugation (3000g) for 5–7 min at 4°. The resulting supernatant was incubated with anti-GFP-protG beads for 30 min at 4° with gentle mixing. The beads subsequently were separated from the supernatant and washed extensively with RB buffer containing

progressively less detergents (0.1% NP-40/0.05% Tween-20). After the final wash, the beads were divided into separate fractions for elution of protein (88% of total) and RNA (12% of total). Protein was eluted in a solution of 0.1% sodium dodecyl sulfate (SDS), 30 mM Hepes (pH 7.4), protease, and RNase inhibitors for 30 min at room temperature. A fraction of the eluted proteins was analyzed immediately by Silver staining (Pierce/ThermoScientific) and Western blot (Licor Odyssey) with the use of a different anti-GFP antibody (catalog no. 632381; Clontech), while the remaining was flash frozen in liquid nitrogen and stored at -80° . The identities of some of the dominant bands on silver stained SDS gels (Figure 1, marked with asterisks) are PB components assigned by their apparent molecular weight by gel migration and MS from other purifications. For RNA isolation, beads were incubated with 1% SDS, 30 mM Hepes (pH 7.4), protease and RNase inhibitors for 30 min at room temperature. The resulting supernatant was mixed with an equal volume of TES buffer [1% SDS in 10 mM Tris (pH 7.5), 1 mM ethylenediaminetetraacetic acid], added to a total equal volume of acid phenol (pH 4), and incubated at 65° for 60 min. Samples were spun at 15,000 *g* for 5 min. Then, the aqueous phase was collected and extracted again with phenol:chloroform, followed by precipitation with cold ethanol. Final pellets were resuspended in TE and stored at -80° .

For I-DIRT experiments, isotopically heavy BY4741 and light Dhh1-GFP frozen cell pellets were ground separately and equal weights of each grindate (to generate 1:1 total protein mass) were mixed immediately before resuspending in RB buffer. The suspension was then cleared by centrifugation and the supernatant collected. Immunoprecipitation with the anti-GFP antibody was performed as described previously.

MS and proteomic analyses

Eluted fractions from the anti-GFP immunoprecipitation (IP) were first precipitated by trichloroacetic acid, then reduced, alkylated, and trypsinized (Promega) (Tian *et al.* 2007). Tryptic digestions were acidified and then desalted by UltraMicroSpin Vydac C18 silica column (Nest Group) following the manufacturer's specifications. Desalted samples were dried and resuspended in a solution of 5% acetonitrile and 0.1% formic acid before tandem mass spectrometric analysis on an LTQ-Velos (for spectral counts) or LTQ-Orbitrap (for I-DIRT) electrospray ionization mass spectrometer.

Tandem mass spectra were converted to universal mzXML file format and searched against a database consisting of all known yeast open reading frames (Saccharomyces Genome Database) (Costanzo *et al.* 2014), known contaminant proteins, and a decoy library prepared by randomization of the library using a Perl script available from the Matrix Science Web site (http://www.matrixscience.com/help/decoy_help.html). Searches were performed by use of the program X!Tandem (Craig and Beavis 2004) with the following parameters: tolerable tryptic termini = 1; identifications based on b- and y-ions; parent mass tolerance = 3.00; fixed modifications include carboxyamidomethylation of cysteine [molecular weight (MW) = 57.02]; and variable modifications include oxidation of methionine (MW = 15.99). Tandem mass spectra peptide and protein assignments were validated by the PeptideProphet (Keller *et al.* 2002) and ProteinProphet (Nesvizhskii *et al.* 2003) programs, available in the current TPP distribution (<http://tools.proteome-center.org/wiki/index.php?title=Software:TPP>). Protein probabilities yielding a 0.05 false-discovery rate threshold were applied to the resulting protein lists and filtered to exclude proteins identified in any experiment with fewer than two unique peptides.

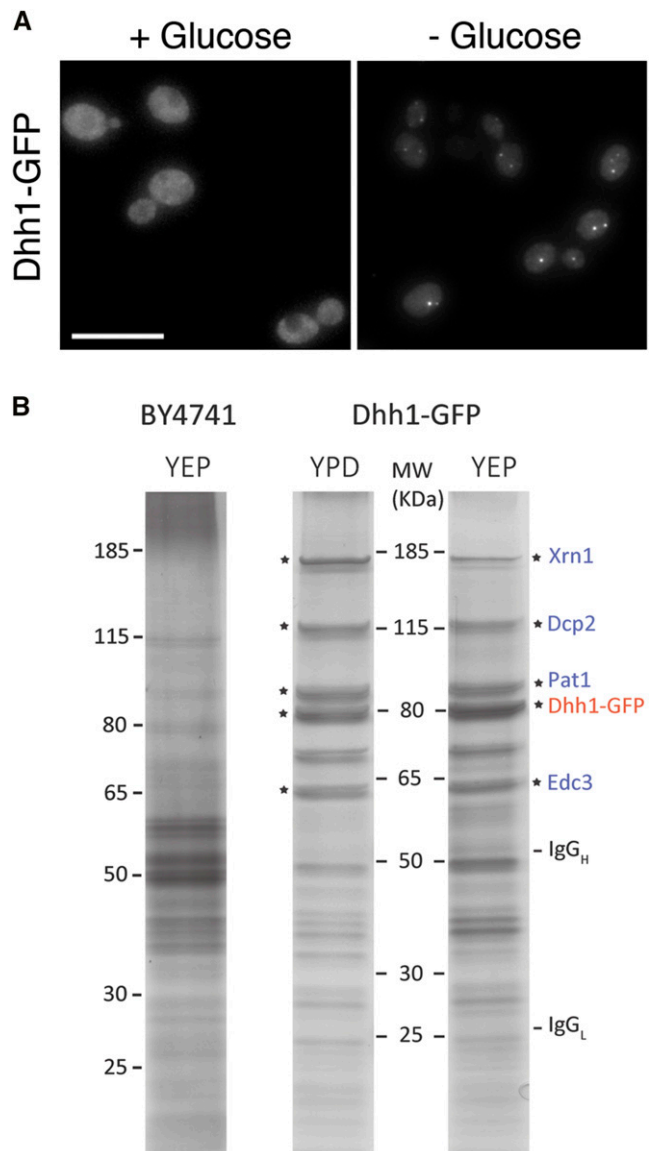


Figure 1 Immunoprecipitation of Dhh1-GFP. (A) Fluorescence microscopy showing the aggregation of Dhh1-GFP into cytoplasmic foci in cells grown in media with and without glucose for 30 min. Scale bar = 10 μ m. (B) Silver stained sodium dodecyl sulfate polyacrylamide gel electrophoresis gels of immunoprecipitation fractions of Dhh1-GFP isolated from cells grown in +glucose (YPD) and -glucose (YEP) media; and from the negative control BY4741 cells grown in -glucose. The identities of some of the dominant bands [marked with an asterisk, Dhh1-GFP (red), and dominant coisolated P-body proteins (blue)] are based on the apparent molecular weight and by mass spectrometry from other purifications. MW, molecular weight of standard proteins.

For spectral count quantitation experiments, paired -glucose and +glucose immunopurified samples were analyzed with two technical replicate injections for each sample on the same mass spectrometer on the same day. Because the number of measured spectra can vary depending on criteria such as protein length or primary sequence, tandem mass spectral counts for each protein identified were normalized using the APEX program (Braisted *et al.* 2008; Vogel and Marcotte 2008) (version 1.1.0) available from the J. Craig Venter Institute Web site (<http://www.jcvi.org/cms/research/software/>). Pre-calculated

observability scores for the yeast proteome (yeast_ORBI_66attrib_ALLpredictions.Oi) were downloaded (http://marcottelab.org/APEX_Protocol/Oi_Predictions/Scerevisiae) and input along with prot.xml files output by the TPP. All proteins lower than the 0.05 false-discovery rate threshold were APEX-normalized, and pairs of –glucose and +glucose samples were compared with the two-sample Z test utility. The APEX-normalized value for each protein was further normalized to the APEX score of the bait Dhh1 from the same immunopurified sample.

To filter proteins known to be common contaminants in GFP affinity purifications, we analyzed and compared our data with control data in the Contaminant Repository for Affinity Purification database (crapome.org) (Mellacheruvu *et al.* 2013). Ten control datasets (Table S2) were selected from experiments that most closely match the experimental approach used in this study: experiments from the S288C strain, affinity purifications using anti-GFP magnetic beads, and proteomics data acquired using LTQ MS. The APEX normalized spectral counts from our data were analyzed along with the spectral counts from the control data sets using the SAINTexpress tool (Mellacheruvu *et al.* 2013) and default analysis parameters. The SAINTexpress algorithm calculates the probability that each protein is likely to be copurified with the bait, and proteins with a SAINT score of 1.0 (Table S2) have strongest probability of being specifically co-enriched with Dhh1–GFP.

To generate the final list of 270 proteins, the following criteria were used: first, only proteins identified in any experiment with more than two unique peptides were considered; second, proteins identified in at least any two of the five + and –glucose experiments (Figure S2); and third, proteins with a SAINT probability score greater than 0.5 in at least one of the two conditions tested, + or –glucose (Table S2). In our +glucose experiments (including two replicates), some proteins are observed to have SAINT scores greater than 0.5 in one replicate, and equal or less than 0.5 in another replicate. Therefore, the final threshold 0.5 SAINT probability score was chosen for all proteins to ensure that each protein must be enriched high enough above the levels in control purifications for at least two replicates per condition. Gene Ontology (GO) category enrichments of the isolated proteins were determined using the YeastMine toolset available from the Saccharomyces Genome Database Web site (<http://yeastmine.yeastgenome.org/yeastmine/>). All reported *p*-values were corrected for multiple hypothesis testing using a Benjamini-Hochberg correction (Benjamini and Hochberg 1995).

The mass spectrometric data from the I-DIRT immunoprecipitated samples were analyzed by the use of a similar approach as described previously with the following differences. Database searches were performed using the following variable modifications: SILAC heavy arginine: ¹³C6-¹⁵N4 (MW = 10.01), and SILAC heavy lysine: ¹³C6-¹⁵N2 (MW = 8.01). After assessment of peptide and protein identifications by PeptideProphet (Keller *et al.* 2002) and ProteinProphet (Nesvizhskii *et al.* 2003), quantitative SILAC ratios for proteins were determined using XPRESS software (Han *et al.* 2001). Precursor ion elution profiles of heavy vs. light peptides were determined with a mass tolerance of 0.05 (>5 sec) and the area under the curve was used to determine a SILAC ratio for each peptide.

Microarray analysis of RNA enrichment

A custom Agilent DNA microarray was designed that consists of 30,529 probes antisense to the *Saccharomyces cerevisiae* transcriptome (Agilent Design ID: 045101). The probes on the array were designed to hybridize to 10,283 different yeast transcripts, including the 6607 ORF transcripts annotated in the SGD as well as 3676 noncoding RNAs. For each transcript, three distinct 60-bp probes were designed and distributed

across the array. In total, seven experiments were assessed by microarray analysis, including RNA extracted from all five preps used to generate protein for MS analysis (described previously), as well as one additional –glucose sample and a mock IP of lysate prepared from a strain expressing GFP alone. For each experiment, a sample of RNA (total RNA) was extracted from cell lysate before immunopurification and compared with RNA extracted from the immunopurified complexes (IP RNA). Then, 5 μg of total RNA and 200 ng IP RNA were fragmented and hybridized per manufacturer's directions to two separate microarrays for each pair of total and IP RNA samples. We used an antibody-based method to directly detect RNA:DNA hybrid on the array (Dutrow *et al.* 2008). The primary S9.6 antibody was purified from hybridoma cell line (ATCC clone HB-8730). Secondary antibody detection was with a Cy3-labeled anti-mouse antibody (catalog no. 078-18-061; KPL). After the final antibody wash, slides were dried by brief, low-speed (600 rpm) centrifugation and immediately scanned. Feature extraction was performed using an Agilent G2565CA Microarray Scanner and control software. The median background signal from 1559 array features designed to have no homology to yeast transcripts was subtracted from all features. Background-subtracted signal was log transformed, pairs of total and IP arrays were normalized by cyclic loess implemented in the Limma Bioconductor package (Smyth 2005), and transcript replicate probes were averaged. Finally, we applied a threshold to remove transcripts that exhibited low abundance signal and high variability or that were saturated on the total RNA array. We generated a linear regression between the average normalized transcript signal in each IP RNA sample and the signal from that transcript in the matched total RNA sample and considered a transcript enriched by the IP if it lay outside the upper 95% confidence interval of the regression line. Microarray design information and data have been deposited with the Gene Expression Omnibus (GEO) database at the National Center for Biotechnology Information under accession no. SE65989.

Microscopy and image analysis

Cells were grown to mid-log phase (OD₆₀₀ ~0.7) in YPD, then pelleted, washed in YEP media without glucose, resuspended in YEP, and grown for another 30 min. Cells were fixed in 2% para-formaldehyde (MeOH free; Polysciences), 10 min at room temperature. Cells were then washed and stored in 1.2M sorbitol/0.1M K-phosphate (pH 7.5). Fixed cells were imaged using a DeltaVision microscope system (Applied Precision, Issaquah, WA), through a 60× oil objective lens in the Olympus IX-71 wide field microscope. Sets of 30, 0.2-μm z-sections were captured for each image, then deconvolved with the use of softWoRx software (Deltavision). Finally, ImageJ software (imagej.nih.gov/ij) was used to adjust contrast levels and images in all the stacks collapsed into one final image.

Data availability

Raw mass spectra (mzML files) are available upon request to the authors. Processed and filtered proteomics data can be found in Table S2, Table S3, and Table S5. Raw and processed microarray data are available at the Gene Expression Omnibus (GEO) database at the National Center for Biotechnology Information under accession number SE65989.

RESULTS

Isolation of PB components

Previous coimmunoprecipitation studies have shown that several core PB components can bind directly to each other even when PB foci are not visible, suggesting that larger PB aggregates could be formed by joining

repeating units of core complex (Decker *et al.* 2007). We set out to identify components that could affect PB aggregation by characterizing proteins that interact with PB core complexes during normal and stress-induced conditions. Due to the dynamic assembly of large PB aggregates, we anticipate that there would be proteins that interact more transiently than others with the PB core complex. Therefore, to optimally capture all interacting components during these dynamic states, we aimed to isolate PB under the mildest possible conditions to best preserve PB integrity. Adapting a comprehensive approach that analyzed the composition of other intact RNP complexes (Oeffinger *et al.* 2007), we developed an immunoaffinity method to isolate the PB core protein Dhh1 at maximal yield. We chose Dhh1–GFP because it is abundant relative to other components (Ghaemmaghami *et al.* 2003), it interacts with several PB components (Coller *et al.* 2001), and it is a component of both yeast PB and SG (Buchan *et al.* 2008; Swisher and Parker 2010). Similar to previous studies, Dhh1–GFP appears cytoplasmically diffuse when cells are grown in media containing glucose but rapidly aggregates into cytoplasmic foci upon an acute stress of glucose depletion (Figure 1A). Cells grown in these two media were rapidly collected by vacuum filtration and flash frozen in liquid nitrogen to minimize induction of PB aggregation during the sample preparation. To best preserve PB subcomplexes and to avoid protein and RNA degradation, cells were lysed in this frozen state by planetary ball mill grinding in liquid nitrogen. Intact Dhh1–GFP foci were observed in the resulting supernatant by fluorescence microscopy. Finally, high yields of Dhh1–GFP complexes (>95% depleted from supernatant) were isolated under native conditions using high affinity anti-GFP antibodies coupled to protein-G magnetic beads.

Silver-stained gels of eluted proteins indicate an enrichment of Dhh1–GFP and associated proteins that are not observed in the control BY4741 sample (Figure 1B). Several core components of the mRNA decay complex (Pat1, Edc3, Dcp2, and Xrn1) copurified with Dhh1 based on their apparent molecular weights. The intensities of these major bands correlate well with their being some of the most abundant proteins in all Dhh1–GFP complexes as measured by mass spectral counts (below).

Proteomic analysis of Dhh1–GFP complexes

To compare PB composition between different cell growth conditions, we analyzed a total of five Dhh1–GFP purifications (two from cells grown in +glucose media, three from –glucose media) by MS. There are a number of proteins that overlap between conditions but are not identified in all replicates of similar condition (*e.g.*, –glucose condition; Figure S2) suggesting that although the profile of major core proteins in Dhh1–GFP complexes appear similar on SDS-polyacrylamide gel electrophoresis, the less-abundant interacting proteins may vary between similar conditions. Therefore, we include in our final list proteins that were identified in any two of the five – and + glucose experiments. In total, we identified 270 proteins that were statistically significant by mass spectrometric analyses (Trans-Proteomic Pipeline; Keller *et al.* 2002; Nesvizhskii *et al.* 2003) and associated with Dhh1–GFP reproducibly in the biological replicates (*Materials and Methods*; Table S2). To filter out proteins that might bind nonspecifically to Dhh1–GFP, we use data from the Contaminant Repository for Affinity Purification to eliminate abundant proteins that have been commonly found to be associated with control GFP-bead IPs (Mellacheruvu *et al.* 2013; *Materials and Methods*, Table S2). Similar approaches have been used to filter common contaminants from yeast (Smith-Kinnaman *et al.* 2014) and mammalian (Wildburger *et al.* 2015) proteomic datasets.

In addition to these five purifications, two SILAC-based purification experiments, termed I-DIRT (Tackett *et al.* 2005), were conducted to further assess *in vivo* protein interactions with Dhh1–GFP. In this approach, coimmunoprecipitated proteins that were labeled with isotopically heavy amino acids from control cells without GFP can only associate with Dhh1–GFP during light- and heavy-labeled extract mixing *in vitro* (*Materials and Methods*). As shown in Figure S1 and Table S3, most PB proteins show strong interactions *in vivo* with Dhh1–GFP, with light:heavy peptide ratios greater than 50:50 (log₂ XPRESS ratio > 0). Interestingly, some known PB components, including Dcp1 and Dcp2, appear to have neutral to low light:heavy peptide ratios, suggesting a dynamic exchange with the isolated Dhh1–GFP complexes, consistent with mammalian studies *in vivo* (Aizer *et al.* 2008). Therefore, we chose not to exclude proteins with light:heavy peptide ratios lower than 50:50, because these might include important components of the complex with dynamic exchange rates. Instead, we considered SILAC light:heavy peptide ratios higher than 50:50 as additional evidence supporting *in vivo* interactions. In total, we found that 130 of the 270 proteins in our final filtered list had SILAC ratios greater than 50:50.

Proteins known to associate with PB

Of the total 270 Dhh1-interacting proteins, 17% have previously been linked to PB and SG (Table 1). Among this set, 16 proteins are considered core components of PB and/or SG (Buchan *et al.* 2010). Most known PB core components were identified (exceptions include the Ccr4/Pop2/Not1 complex and Scd6), and relative to all proteins co-isolated with Dhh1–GFP, the family of decapping proteins Dcp1, Dcp2, Edc3, Pat1, Lsm1-7, and exonuclease Xrn1, were the most abundant PB proteins (highest spectral counts) isolated from cells grown either in –glucose or +glucose media (Table S2). Similar to the SDS-polyacrylamide gel electrophoresis profile (Figure 1), the stoichiometry among these 12 core proteins relative to each other and to Dhh1 appeared very similar in both growth conditions, suggesting that an inherent Dhh1 core subcomplex exists regardless of the induction status of PB/SG foci. These results are consistent with previous studies showing that several core PB components, including Dhh1, can bind directly to each other by *in vitro* pull-down assays and can be coimmunoprecipitated even from cells grown in glucose supplemented media (Tharun *et al.* 2000; Coller *et al.* 2001; Kshirsagar and Parker 2004; Decker *et al.* 2007; Harigaya *et al.* 2010). Notably Lsm1, and not Lsm8, was identified along with the Lsm2-7 proteins in all of the purification replicates. Lsm1 binds to Lsm2-7 proteins and forms a cytoplasmic decapping complex that associates with PB, whereas Lsm8 forms another complex with Lsm2-7 that is recruited to the nucleus to perform splicing and processing of nucleolar and ribosomal RNA (Novotny *et al.* 2012). The absence of Lsm8 from our purifications suggests a preferential association of cytoplasmic Lsm1-7 complexes with Dhh1–GFP. Core SG proteins that interact with Dhh1–GFP (Cdc33, Pab1, Pbp1, Tif2) were also identified, but at lower abundance (by spectral counts) than core PB proteins (Table S2). Finally, 31 coisolated proteins are considered PB/SG-associated (Table 1) because they colocalize partially with PB/SG core proteins, or they affect PB/SG assembly (Balagopal and Parker 2009; Buchan and Parker 2009; Tkach *et al.* 2012; Buchan *et al.* 2013; Yang *et al.* 2014). Because of the dynamic interchange of components between PB and SG foci, we will henceforth denote Dhh1–GFP binding proteins as PB/SG. Thus, our results provide biochemical evidence for several proteins that were previously associated with PB or SG by only colocalization or genetic studies.

■ **Table 1 Known PB and SG components coisolating with Dhh1-GFP**

Category	References
Core PB/SG ^a	
Dcp1, Dcp2, Lsm1-7, Pat1, Xrm1	(Sheth and Parker 2003)
Cdc33 (eIF4E)	(Bregues and Parker 2007; Hoyle <i>et al.</i> 2007; Grousl <i>et al.</i> 2009)
Edc3	(Kshirsagar and Parker 2004; Decker <i>et al.</i> 2007)
Pab1	(Bregues and Parker 2007; Hoyle <i>et al.</i> 2007)
Pbp1	(Buchan <i>et al.</i> 2008)
Tif2 (eIF4A)	(Buchan <i>et al.</i> 2011)
PB/SG-associated Condition-specific colocalization ^b	
Edc1	(Dunckley <i>et al.</i> 2001)
Fun12 (eIF5b)	(Buchan <i>et al.</i> 2011)
Hrr25	(Shah <i>et al.</i> 2014)
Lsm12, Pbp4	(Swisher and Parker 2010)
Nab6, Sro9	(Mitchell <i>et al.</i> 2013)
Nam7	(Sheth and Parker 2006)
Prt1 (eIF3b), Rpg1 (eIF3a)	(Grousl <i>et al.</i> 2009; Buchan <i>et al.</i> 2011)
Puf3	(Lee <i>et al.</i> 2009; Mitchell <i>et al.</i> 2013)
Rpm2	(Stribinskis and Ramos 2007)
Sbp1	(Segal <i>et al.</i> 2006; Mitchell <i>et al.</i> 2013)
Sup35 (eRF3)	(Gilks <i>et al.</i> 2004; Buchan <i>et al.</i> 2008; Grousl <i>et al.</i> 2013)
Tef4 (eEF1Bg), Yef3 (eEF3)	(Grousl <i>et al.</i> 2013)
Vma2	(Buchan <i>et al.</i> 2013)
Ssa2, ^c Sis1, ^c Ydj1 ^c	This study; (Walters <i>et al.</i> 2015)
Genetic and/or biochemical interactions with PB/SG proteins; no colocalization data	
Atp1, Cdc48, ^d Def1, Yra1	(Weidner <i>et al.</i> 2014)
Hsp104, Mkt1	(Tkach <i>et al.</i> 2012)
Stm1	(Balagopal and Parker 2009)
Ubp3 ^d	(Rinnerthaler <i>et al.</i> 2013)
Affects assembly; no colocalization data	
Asc1 ^d	(Arimoto <i>et al.</i> 2008; Tkach <i>et al.</i> 2012)
Gsp1, Sse1	(Yang <i>et al.</i> 2014)

Alternate names are listed in parentheses; PB, P-body; SG, stress granule.

^a Conserved in yeast and mammals; constitutive localization; in many cases, PB and SG proteins overlap in the same foci.

^b Localization to PB/SG depending on stress conditions, in certain mutants, or overexpressing conditions.

^c Affects assembly/disassembly of PB/SG.

^d Only mammalian homolog shown to colocalize with mammalian core proteins.

One of the most enriched categories of cellular components from our list of 270 Dhh1-associated proteins was a set of ribosomal proteins (structural constituent of ribosome, 81 total; hypergeometric p -value = 1×10^{-44}). This result is consistent with several studies showing a close association between ribosomes and PB components, including Dhh1 (Kressler *et al.* 1997; Bonnerot *et al.* 2000; Hu *et al.* 2009; Drummond

et al. 2011; Sweet *et al.* 2012; Cougot *et al.* 2012). Components of both the 40S and 60S subunits were identified, including Rps30A and Rpl16A (Table S2), which have been reported to bind Dhh1 (Drummond *et al.* 2011; Sweet *et al.* 2012). More than 35% ($n = 94$; Table S4) of the Dhh1-GFP-interacting proteins are nonribosomal RNA-binding proteins (RBP) that are part of RNP granules ($P = 2 \times 10^{-17}$) (PB and SG) and RNP complexes ($P = 2 \times 10^{-52}$). These include other preribosomal, polysomal, nucleolar, and translation associated proteins (Figure 2A, Table S4). In addition to their known targets of ribosomal RNAs (rRNAs), transfer RNAs (tRNAs), or small nucleolar RNAs for ribosome biogenesis, or their role in other cellular functions such as vacuolar trafficking or glycolysis, many of the 94 nonribosomal RBP have recently been found to bind mRNA (Hogan *et al.* 2008; Scherrer *et al.* 2010; Tsvetanova *et al.* 2010; Mitchell *et al.* 2013). Thus, affinity purifying Dhh1 under native condition has allowed us to isolate the core PB subcomplexes along with many PB/SG associated proteins known for their role in mRNA binding and translational functions.

Metabolic enzymes, tRNA synthases, and protein chaperones

In addition to known RNA granule, ribosomal, and RNA binding-proteins, the 189 nonribosomal proteins were enriched for several other functional classes. One class included proteins associated with metabolic and biosynthetic processes, in particular proteins annotated as binding ATP (*e.g.*, “nucleobase-containing small molecule metabolic process,” $P = 7 \times 10^{-18}$) (Figure 2A). Approximately 43% of the proteins included in this latter GO category are also RBP (Table S4). Other related GO processes include cellular amino acid metabolism ($P = 8 \times 10^{-12}$), glycolysis ($P = 4 \times 10^{-7}$), protein folding ($P = 6 \times 10^{-4}$), and tRNA aminoacylation ($P = 2 \times 10^{-8}$). Because proteins in these classes have been shown to localize to cellular foci in response to stresses such as DNA replication inhibition, acute glucose depletion, and stationary phase starvation (Narayanaswamy *et al.* 2009; Tkach *et al.* 2012; Mitchell *et al.* 2013), we wondered how many of our 270 Dhh1-associated proteins had evidence of stress-dependent localization to cellular foci. Of our 270 Dhh1-GFP-associated proteins, 55 had been reported in the literature to form foci in at least one of the three stress conditions (Table S6). These included 27 of the known PB/SG components in our list. Of the remaining 28 Dhh1-GFP interactors that had not previously been shown to colocalize with PB/SG proteins, 24 proteins, including metabolic enzymes, tRNA synthetases, and protein chaperones, had been shown to form foci only in stationary phase cells. Taken together, these findings suggest that a subset of proteins that respond to stress by relocalizing to foci interact with Dhh1-GFP and are thus new candidates for PB/SG-associated components.

Proteins that preferentially associate with Dhh1-GFP in the PB-induced state

To compare the composition of the Dhh1 complex in the two different cell growth conditions, we analyzed pairs of Dhh1-GFP immunoprecipitations from -glucose and +glucose media detected by MS using the same instrument on the same day to reduce technical variability. We used the APEX program (Braisted *et al.* 2008; Vogel and Marcotte 2008) to determine the normalized spectral count for each protein as an indication of their relative abundance in the protein purification (*Materials and Methods*). APEX spectral count scores for each protein were further normalized to the APEX spectral count of Dhh1-GFP itself measured in the same sample, and the ratio of normalized scores from pairwise -glucose to +glucose samples was generated as a measure of the extent to which each protein is preferentially associated with Dhh1-GFP in the -glucose condition (PB induced) (Table S5). Of all

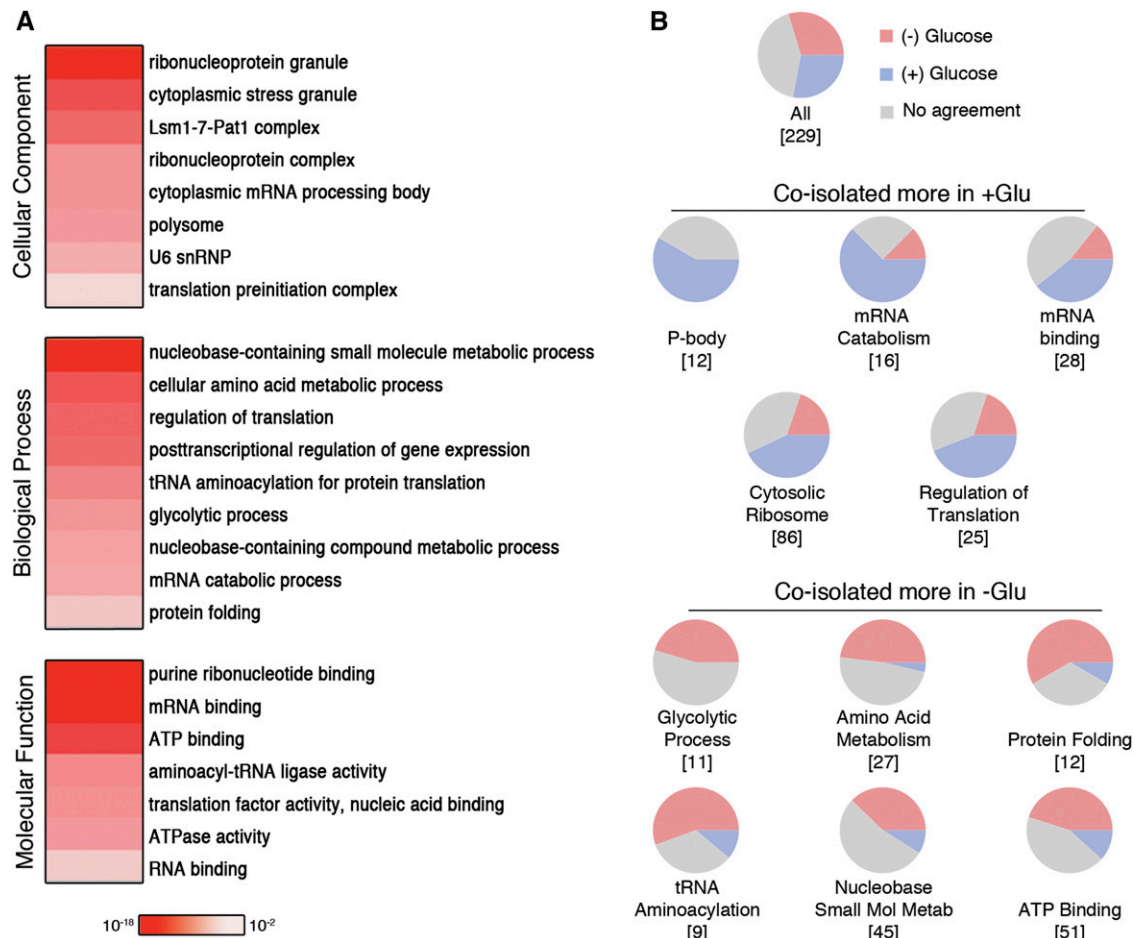


Figure 2 Protein constituents of Dhh1-GFP complexes. (A) Gene ontology (GO) enrichment represented as heatmap of 189 nonribosomal Dhh1-GFP-interacting proteins. Color intensity corresponds to the p -value from the hypergeometric test after correcting for multiple hypothesis testing. (B) Condition-specific coisolation of protein subsets with Dhh1-GFP. Pie charts show the proportion of proteins in each GO category that reproducibly change in abundance when coisolated with Dhh1-GFP from different growth conditions. Protein abundance was determined by the use of APEX-normalized spectral counts and further normalized to the level of Dhh1-GFP. Proteins that are reproducibly more abundant when coisolated with Dhh1-GFP from cells grown in +glucose are shown in blue, those reproducibly more abundant when coisolated from cells grown in -glucose are shown in red, or where there is no agreement between replicates in gray. The total number of proteins from each category measured in both spectral count experiments is indicated in square brackets.

pairwise comparisons, 64 proteins had scores consistent with higher levels in the +glucose condition and 68 proteins had scores consistent with higher levels in the -glucose condition. The set of proteins predicted to be associated with Dhh1 more in the +glucose condition had significant enrichment for the GO categories of RNA catabolism, regulation of translation, and ribosome. In contrast, those predicted to associate at higher levels in the -glucose condition (PB induced) were significantly enriched for glycolysis, amino acid metabolism, protein folding, tRNA aminoacylation (tRNA synthetases), and ATP-binding (Figure 2B). These results suggest that the induced state of PB tends to accumulate similar classes of PB/SG components that respond to stress by relocating to foci.

We further examined the condition-specific association of each protein to Dhh1-GFP by using APEX scores described previously (Table S5) with their SAINT probability scores calculated separately for each growth condition (Table S2). Of the proteins already shown to be preferentially enriched in either -glucose or +glucose by APEX score analyses, we further filtered for those with SAINT scores greater than 0.6 in one condition of the same trend and lower than 0.4 in the other

(Table 2). In total, 16 proteins are coisolated more with Dhh1-GFP in the -glucose condition and six in the +glucose condition. Of note, the SG core protein Cdc33 is only coisolated with Dhh1-GFP in the -glucose condition, consistent with previous SG colocalization studies (Swisher and Parker 2010). This filtered list reveals similar GO-annotated classes of proteins as the larger list from Figure 2B including proteins involved in amino acid metabolism, tRNA synthetases, and protein folding.

Enrichment of proteins with LC and prion domains in yeast RNP granules

Studies in mammalian cells have identified LC regions as a common feature of many RBP and demonstrated the importance of these regions for both RNP granule aggregation and RNA retention (Han *et al.* 2012; Kato *et al.* 2012; Castello *et al.* 2012). We tested whether our set of Dhh1-associated proteins contained LC domains by two orthogonal approaches. First, we searched the set of 5887 ORFs annotated in the yeast genome database for LC sequences of at least 35 residues using the SEG algorithm (Wootton 1994) and found that 390 proteins meet these

■ **Table 2** Proteins coisolated with Dhh1–GFP in specific conditions

Protein	Conditional Enrichment (APEX Scores) ^a	SAINT Probability Scores ^b		GO Category ^c	Biological Functions
		–Glu	+Glu		
Bat1	–Glu	1.00	0.00	Amino acid metabolism	Mitochondrial branched-chain amino acid (BCAA) aminotransferase
Gln1	–Glu	1.00	0.00	Amino acid metabolism	Glutamine synthetase (GS)
Hom6	–Glu	0.67	0.00	Amino acid metabolism	Homoserine dehydrogenase (L-homoserine:NADP oxidoreductase)
Met6	–Glu	1.00	0.00	Amino acid metabolism	Cobalamin-independent methionine synthase
Ura2	–Glu	0.70	0.00	Amino acid metabolism	Bifunctional carbamoylphosphate synthetase/aspartate transcarbamylase
Ahp1	–Glu	1.00	0.00	Antioxidant activity	Thiol-specific peroxidoredoxin
Cdc48	–Glu	1.00	0.00	ATP binding	AAA ATPase
Sec31	–Glu	1.00	0.00	COPII vesicle coat	Component of the Sec13p-Sec31p complex of the COPII vesicle coat
Ipp1	–Glu	1.00	0.00	Nucleobase small mol metab	Cytoplasmic inorganic pyrophosphatase (PPase)
Ssb2	–Glu	0.67	0.00	Protein folding	Cytoplasmic ATPase that is a ribosome-associated molecular chaperone
Tsa1	–Glu	0.67	0.00	Protein folding	Thioredoxin peroxidase
Ydj1	–Glu	0.65	0.00	Protein folding	Type I HSP40 co-chaperone
Cdc33	–Glu	0.67	0.00	Stress granule	mRNA cap binding protein and translation initiation factor eIF4E
Dps1	–Glu	1.00	0.00	tRNA aminoacylation	Aspartyl-tRNA synthetase, primarily cytoplasmic
Krs1	–Glu	0.67	0.00	tRNA aminoacylation	Lysyl-tRNA synthetase
Mes1	–Glu	1.00	0.00	tRNA aminoacylation	Methionyl-tRNA synthetase
Ask10	+Glu	0.33	0.98	Glycerol transport	Regulator of the Fps1p glycerol channel
Pet130	+Glu	0.33	1.00	Mitochondrion	Protein required for respiratory growth
Rrg1	+Glu	0.33	1.00	Mitochondrion	Protein of unknown function; Required for Respiratory Growth
Dbp3	+Glu	0.24	0.56	Ribosome biogenesis	RNA-Dependent ATPase, member of DExD/H-box family
Nop2	+Glu	0.33	0.91	Ribosome biogenesis	rRNA m5C methyltransferase
Rpc40	+Glu	0.40	0.99	Ribosome biogenesis	RNA polymerase subunit AC40

GO, Gene Ontology.

^a From Table S5.

^b From Table S2.

^c Same as in some of the GO categories listed on Figure 2.

criteria (Table S7). Similar to the findings in mammalian systems (Kato *et al.* 2012), these proteins are strongly enriched for mRNA binding functions ($P = 3 \times 10^{-10}$) and regulation of gene expression (2×10^{-13}). Second, we considered a set of 178 yeast proteins predicted by Alberti *et al.* (2009) that contain putative prion-like domains. Protein–protein interactions via prion-like Q/N-rich domains, a specialized class of LC domains, have been shown to be essential for PB and SG aggregation (Gilks *et al.* 2004; Decker *et al.* 2007; Reijns *et al.* 2008). Both lists (390 LC and 178 prion) share 72 proteins in common ($P = 1.6 \times 10^{-44}$), suggesting that these approaches identify similar protein sequence features (Table S7).

Of the 390 proteins predicted to contain LC domains, 25 were coisolated with Dhh1–GFP ($P = 9 \times 10^{-3}$). Of the 178 proteins predicted

to contain putative prion domains, 18 were coisolated with Dhh1–GFP ($P = 1 \times 10^{-4}$). In total, we found that 35 Dhh1–GFP interactors contained predicted LC or prion-like domains, including 8 proteins that were in both sets. Of these 35 proteins, 24 are known RBP and the most significantly enriched GO categories include mRNA binding, RNP granule, and RNP complex (Table S7). These results are consistent with mammalian studies demonstrating that proteins containing LC regions are highly represented in yeast RNP granules such as PB and SG.

Ydj1 regulates Dhh1–GFP foci formation under acute glucose depletion stress

We identified 17 protein chaperones that coisolate with Dhh1–GFP, including components of the CCT/TRiC chaperonin complex and

members of the Hsp40, Hsp70, and Hsp90 families. Members of these chaperone families have been shown to be involved in PB/SG assembly by regulating the interactions between Q/N domain proteins and prion proteins (Gilks *et al.* 2004; Rikhvanov *et al.* 2007; Matsumoto *et al.* 2011; Nadler-Holly *et al.* 2012). Given that a significant number of proteins co-isolating with Dhh1-GFP also contain putative LC/prion domains, we tested whether any of the chaperones identified might be involved in regulating the aggregation of PB/SG foci. Because protein chaperones as a group are also associated with Dhh1-GFP at a higher level in cells grown in -glucose media (PB-induced condition) (Figure 2B), we focused on this condition.

The Hsp40 family protein Ydj1 has an LC domain (Table S7), binds Q/N-prion domain proteins (Summers *et al.* 2009), and in our proteomic studies associates with Dhh1-GFP only in the glucose depleted condition (Table 2 and Table S5). To test the effects of Ydj1 on PB assembly, we examined the ability of Dhh1-GFP, Lsm1-GFP or Edc3-GFP to localize to cytoplasmic foci in a *ydj1Δ* mutant background. In contrast to wild-type cells, Dhh1-GFP or Lsm1-GFP foci formation are defective in *ydj1Δ* mutant cells that are grown in glucose-depleted media (Figure 3A). The formation of Dhh1-GFP or Lsm1-GFP foci when cells were grown to saturation, another PB inducing condition, also was drastically reduced in the *ydj1Δ* mutant background. In contrast, the loss of *YDJ1* had minimal effects on Edc3-GFP aggregation (Figure 3A). We also tested whether deletion of other members of the Hsp70, Hsp90 and Hsp110 families, including *ssa1Δ*, *ssa2Δ*, *hsc82Δ*, *hsp82Δ*, or *hsp104Δ*, affected the stress induction of Dhh1-GFP foci and found that Dhh1-GFP foci formation to be the same as wild-type in all these mutant backgrounds (Figure S3). The Dhh1-GFP foci assembly defect in *ydj1Δ* mutant (YAD557) was complemented by plasmids containing a wild-type copy of *YDJ1*, but not any of the other related protein chaperones tested (Figure 3, B and C). We also examined the effects of the *ydj1Δ* mutation on protein levels of Dhh1-GFP, Lsm1-GFP or Edc3-GFP, and found that in all three cases the protein levels are decreased to about 20% of the levels in wild-type cells (Figure S4A). Reintroducing the wild-type *YDJ1* did not restore Dhh1-GFP level to that of wild-type (Figure S4B). This result suggests that the interplay between *YDJ1*, protein levels, and RNA granule assembly is complex and not fully resolved by these experiments. The interpretation of these data may be confounded by the differences between the expression of *YDJ1* from the plasmid vs. the endogenous chromosomal locus. Furthermore, there may be a residual epigenetic effect of the deletion of *ydj1* that has not been addressed by the complementation; Ydj1 is known to be central in prion formation and propagation (Summers *et al.* 2009). It is also possible that when wild-type *YDJ1* is introduced, the levels of Lsm1 or Edc3 in the *ydj1Δ* strain that expresses Dhh1-GFP are restored enough to drive Dhh1-GFP foci assembly. Taken together, these results suggest that Ydj1 is required for the formation of Dhh1- and Lsm1-containing cytoplasmic foci in response to glucose limitation stress.

Analysis of RNA associated with Dhh1-GFP complexes

Because PB are known to depend on the presence of RNA for their integrity (Teixeira *et al.* 2005), we isolated RNA in parallel from each Dhh1-GFP immunopurified samples analyzed by MS. To facilitate the quantification of strand-specific transcripts in a manner that was independent on their polyadenylation status and not biased by the amplification protocol, we hybridized RNA directly to a custom DNA microarray and measured RNA abundance by using an antibody specific for RNA:DNA hybrids (Hu *et al.* 2006; Dutrow *et al.* 2008). Transcripts were considered enriched in the IP if they were above the 95% confidence interval of a linear regression between the normalized signal

from matched IP and total RNA samples (Figure 4A). Using this method, we identified 79 transcripts that copurified with Dhh1-GFP in more than one biological replicate but not in the mock sample which immunoprecipitated GFP alone (Table S8). The majority of these 79 transcripts are significantly enriched for noncoding RNAs, including dubious ORF transcripts, cryptic unannotated transcript, stable unannotated transcript (Xu *et al.* 2009), and meiotic unannotated transcript (Lardenois *et al.* 2011) (Figure 4B). We also detect evidence of enrichment of Ty retroelements, along with proteins encoded by Ty elements, consistent with Ty association with PB (Checkley *et al.* 2010). Although the majority of identified transcripts are noncoding, we did not detect coenrichment of related transcripts, *e.g.*, pairs of sense and antisense transcripts, which would suggest a regulatory role.

Interestingly, the most enriched transcript in every Dhh1-GFP IP replicate is the mRNA encoding the PB protein Pat1 (Figure 4 and Figure S5B). mRNA encoding Dcp2 is also enriched, but not to the same extent as the *PAT1* mRNA (Figure 4A). Pat1 and Dcp2 are among the most abundant PB proteins in the Dhh1-GFP purification. Coenrichment of both protein and mRNA could occur if nascent translation products remain associated with the mRNA on polysomes or if the protein regulates its cognate transcript (Pullmann *et al.* 2007). Of all the 270 Dhh1-GFP-interacting proteins, only nine mRNAs are found together with their cognate proteins in the same IP replicate (Figure S6), suggesting that transcripts generally are not isolated together with their cognate proteins in these IPs. Pat1 is unique among the PB core proteins in that it can be shuttled between the nucleus to cytoplasm, and this localization depends on associating with PB proteins Lsm1 and Dhh1 (Teixeira and Parker 2007; Hurto and Hopper 2011; Bahassou-Benamri *et al.* 2013), suggesting Pat1 has a nuclear function that may not be directly associated with PB. This finding would be consistent with the behavior of the vertebrate paralog Pat1a, which localizes poorly to PB and has a separate function from the more conserved Pat1b protein (Marnef and Standart 2010). Although the data presented here neither confirm nor refute the hypothesis, the substantial enrichment of *PAT1* mRNA suggests that this transcript itself could play a role in PB assembly, function, or stability through a structural or catalytic activity.

The next most highly enriched RNA is the *RPM1* transcript, which is the catalytic RNA component of mitochondrial RNase P (Sulo *et al.* 1995). Although this RNA-protein complex has a well-characterized mitochondrial function, we detected both *RPM1* and the protein component of the mitochondrial RNase P, Rpm2, in four of our six Dhh1-GFP IP samples. These results are also consistent with previous observations that the Rpm2 protein localizes to PB and genetically interacts with PB components (Stribinskis and Ramos 2007). Among the noncoding elements, two distinct classes of mitochondrially encoded ribozymes also are identified and confirmed by quantitative reverse transcription polymerase chain reaction (qRT-PCR) (Figure S5), including several self-splicing introns from the *COX1* and *21S* rRNA loci (*AI3*, *AI4*, *AI5α*, and *SCEI*). Only the DEAD-box helicase Mss116 that facilitates *in vivo* splicing of mitochondrial introns (Huang *et al.* 2005; Solem *et al.* 2006) is detected among the RBP coisolating with Dhh1-GFP, whereas another mitochondrial helicase Suv3, involved in mitochondrial RNA decay, is not (Borowski *et al.* 2010; Bruni *et al.* 2012; Szczesny *et al.* 2013). Thus, PB/SG foci are enriched for a set of well-characterized, noncoding RNAs with catalytic activity along with their associated RBPs.

DISCUSSION

Here, we have used a high-affinity antibody to isolate core Dhh1-GFP complexes at maximal yield under conditions that preserve the PB aggregate state. The method has allowed us to reproducibly isolate

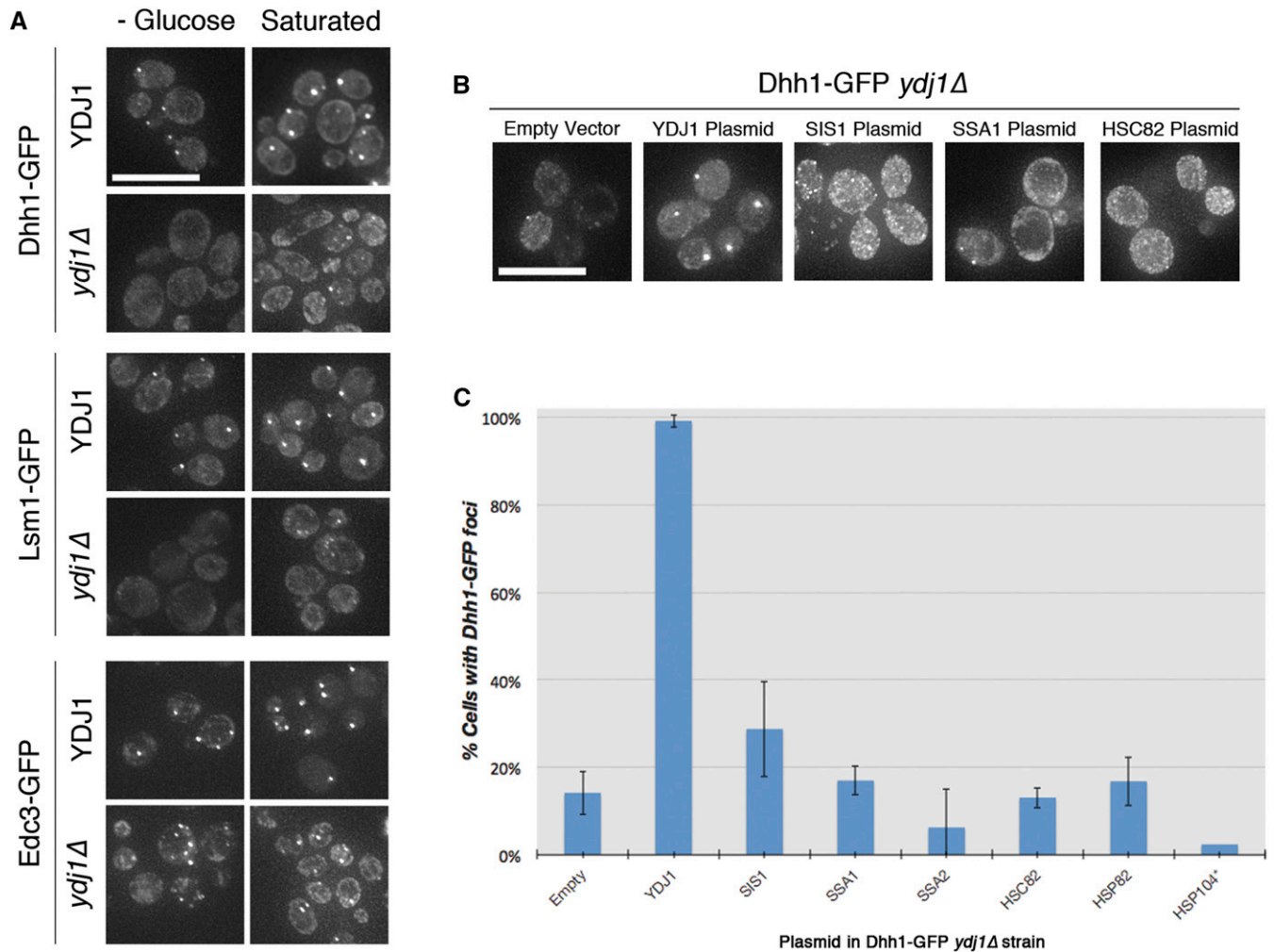


Figure 3 Ydj1 is necessary for the formation of PB foci. (A) Fluorescence microscopic images of Dhh1–GFP, Lsm1–GFP, or Edc3–GFP in wild-type (YDJ1) or mutant (*ydj1Δ*) cells after a 30-min glucose depletion, or overnight culture. Scale bar = 10 μ m. (B) Microscopic images of Dhh1–GFP in *ydj1Δ* mutants transformed with centromere-containing plasmids harboring the corresponding genes. All strains were induced to form foci by 30 min of glucose depletion. Scale bar = 10 μ m. (C) Quantitation of the percent of cells with at least 2 Dhh1–GFP foci after 30 min of glucose depletion for the strains in (B). Data presented are the average of at least two replicate experiments in which a minimum of 40 cells were counted. Error bars represent the standard deviation of the replicate measurements. (*only 1 replicate quantified for Hsp104.)

PB core components at level stoichiometric to that of the bait Dhh1–GFP as well as a number of PB/SG accessory proteins. Our results provide biochemical evidence for a number of proteins that have only been associated partially with PB/SG foci under certain conditions, or implicated in controlling PB/SG assembly by genetic studies without localization data (Buchan *et al.* 2013; Yang *et al.* 2014). SG proteins also copurify with Dhh1–GFP, but at lower abundance than known PB proteins. Our results support the model of a continuum of mRNP granules transitioning between PB and SG foci, particularly during stress (Grousl *et al.* 2009; Buchan and Parker 2009). We expect that more proteins from our list might be identified to be functionally associated with Dhh1 in other genetic screens (*e.g.*, overexpressing or deletion mutants), since many proteins that regulate PB/SG function do not have well characterized RNA metabolism or translational regulatory activities (Buchan *et al.* 2013; Yang *et al.* 2014).

LC-containing proteins and role of chaperones in regulating PB aggregation

PB formation is a dynamic process between mRNP granule assembly and disassembly states during a stress response (Buchan 2014). In

mammalian cells, a high proportion of RNA-binding proteins found in RNP granules contain LC domains that are necessary and sufficient to transform RNP complexes from soluble to aggregate states (Kato *et al.* 2012). In a similar trend, 13% of the proteins in our PB enrichment are predicted to have LC/prion domains with more than two thirds being RBP. Furthermore, subgroups of protein chaperones (*i.e.*, heat-shock-proteins) are selectively enriched with Dhh1–GFP in the PB-inducing condition of low glucose. Various heat shock proteins have been localized to SG and are required for disassembly and the reinitiation of translation upon removal from stress (Cherkasov *et al.* 2013; Buchan 2014). Prion studies also have shown that factors controlling prion protein aggregation depend on protein concentration, an organizing scaffold, and a network of chaperones (Summers *et al.* 2009). We show here that the Hsp40 chaperone Ydj1, which can bind to prion domains and also has a predicted LC domain, is specifically required for Dhh1–GFP foci assembly. Ydj1 is part of the Hsp40-70-110 chaperone network that regulates the aggregation–disaggregation of yeast prion proteins (Summers *et al.* 2009). The fact that Ydj1 affects PB formation strongly supports the model that Ydj1 mediates LC/prion

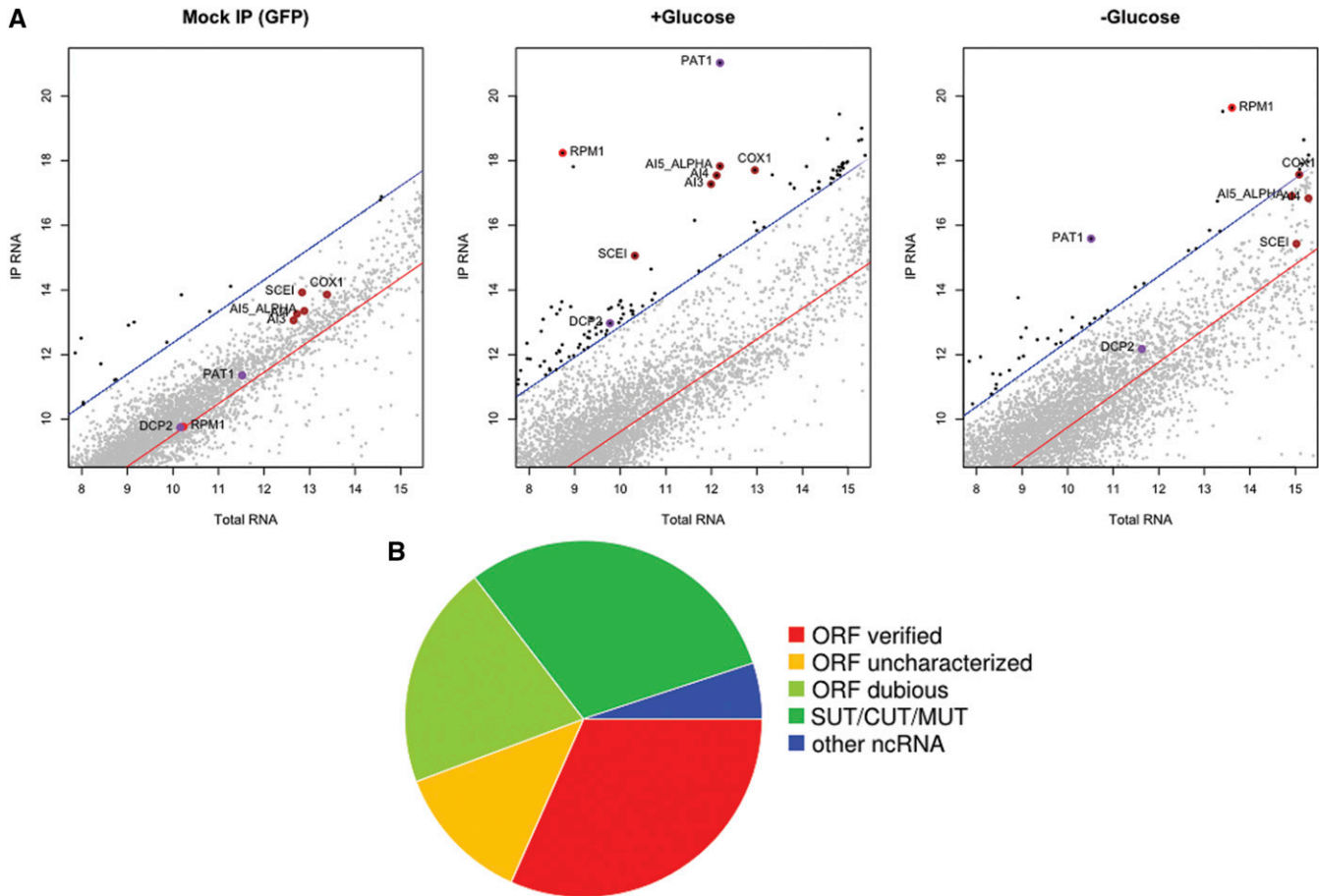


Figure 4 Analysis of RNA isolated in Dhh1–GFP complexes. (A) Representative microarray data from a mock immunoprecipitation (IP; green fluorescent protein alone) as well as Dhh1–GFP immunoprecipitations from a +glucose and a –glucose condition. The x-axis in each plot is the log-transformed, normalized array intensity for input (total) RNA, and the y-axis is the log-transformed, normalized array intensity for IP RNA. In each plot, the red line is a linear regression between the signals from the IP and total RNA, and the blue lines correspond to the 95% confidence interval. Transcripts above 95% confidence interval are considered enriched (and shaded black). Specific transcripts that are enriched and discussed in the text are highlighted and labeled (red, *RPM1*; brown, mitochondrial introns; purple, *PAT1* and *DCP2*). (B) The proportion of each RNA class within the total identified 79 transcripts. ORF, open reading frame; SUT, stable unannotated transcript; CUT, cryptic unannotated transcript; MUT, meiotic unannotated transcript.

domain interactions among RNP proteins to assemble PB. The accumulation of unfolded proteins during stress could affect the level of various chaperones in cells and drive the equilibrium toward aggregation of LC proteins into PB/SG (Buchan and Parker 2009; Buchan 2014). This model could explain why overexpression of Ydj1 alone does not cause Dhh1–GFP foci formation in the absence of an acute glucose stress. Ydj1 might affect PB assembly only by coordinating its activity with other co-chaperones, and without a stress trigger, the chaperone network equilibrium is not perturbed.

Because levels of Dhh1, Edc3, and Lsm1–GFP are found to decrease in the *ydj1Δ* mutant, the assumption might be that a critical concentration of one of these core proteins is required to drive PB aggregation. However, reintroducing wild-type *YDJ1* rescued the Dhh1–GFP foci assembly defect but did not restore Dhh1–GFP protein level to that of wild-type. Because PB assembly appears to be a redundant process and occurs even when certain PB core proteins are deficient (Sheth and Parker 2003), the possibility remains that overexpressing *YDJ1* has restored the level of other PB proteins sufficiently to drive PB assembly. Furthermore, because Dhh1–GFP foci are still observed in some *ydj1Δ* cells grown to stationary phase, and Edc3–GFP foci are diminished but

not completely missing in *ydj1Δ* cells exposed to glucose stress, there are likely multiple factors controlling PB/SG assembly. During the preparation of this manuscript, (Walters *et al.* 2015) show that members of the Hsp70 (*Ssa1*, 2, and 4) and Hsp40 (*Ydj1* and *Sis1*) families colocalize with SG foci during azide stress induction. These results corroborate with our studies as *Ssa2* and *Sis1* are coisolated with Dhh1–GFP in addition to Ydj1. However, Ydj1 and *Sis1* are observed to be involved in SG disassembly after stress removal in their studies (using *Pab1* and *Ded1* as markers), rather than PB assembly as in our studies (using *Dhh1* and *Lsm1* as markers). Notably, Ydj1 and *Sis1* have different effects on SG disassembly, similarly to their different effects on PB assembly observed in our studies, confirming that different Hsp40 proteins play different roles in PB/SG assembly/disassembly.

PB/SG and protein foci formation in response to stress

An important clue for understanding the relevance of Dhh1–GFP-associated proteins with PB functions is the strong overlap with proteins that redistribute to cytoplasmic foci in response to various environmental stress (Narayanaswamy *et al.* 2009; Tkach *et al.* 2012; Shah *et al.* 2014). Transient protein aggregation is a physiological

means to triage proteins for refolding or degradation (Escusa-Toret *et al.* 2013; Sontag *et al.* 2014). Major protein subgroups that are associated more with Dhh1–GFP in the PB induced state (*e.g.*, chaperones, metabolic enzymes involved in amino acid/purine synthesis, tRNA synthetases) also form foci in stationary phase cells. The majority of these proteins form aggregates that are reversible, suggesting that they are not permanently denatured protein aggregates (Narayanaswamy *et al.* 2009). Protein granules observed in stationary-phase cells are associated with a network of chaperones that are very similar to those we see associated with Dhh1–GFP (O’Connell *et al.* 2014). Cells might assemble metabolic enzymes into foci to modulate their activities, to provide structural stability, or to concentrate metabolites and RNA into transient storage in order to quickly re-enter the cell cycle once stress is removed (O’Connell *et al.* 2012). Most of the proteins in our isolations that form foci also bind ATP (*i.e.*, metabolic enzymes and tRNA synthetases), and almost half also bind RNA. According to the REM hypothesis (Scherrer *et al.* 2010; Hentze and Preiss 2010), metabolic enzymes that bind to mRNA as well as metabolites such as ATP can provide cells a mechanism to link post-transcriptional regulation with cellular metabolism. Cells might be able to enhance long-term survival by allowing metabolic enzymes the ability to quickly adapt to binding mRNA when substrate availability is limited during starvation. Finally, a subgroup of tRNA synthetases is coprecipitated with the foci-forming tRNA synthetase IIs1-GFP in stationary phase cells (O’Connell *et al.* 2014) very similarly with the tRNA synthetase subgroup that interacts with Dhh1–GFP in acute glucose depletion. Regulation of the nuclear tRNA pool has been shown to be coordinated with PB assembly in response to amino acid starvation in yeast (Hurto and Hopper 2011). A current model suggests that cells modulate the aminoacyl-tRNA repertoire to regulate preferential translation of certain proteins during stress (Subramaniam *et al.* 2014) or during cell proliferative state (Gingold *et al.* 2014).

RNA associated with Dhh1–GFP complexes

The reproducible isolation of subsets of RBP in our PB enrichment allows us to characterize the associated transcripts specific to Dhh1–GFP subcomplexes. The strikingly strong enrichment of *PAT1* and *RPM1* transcripts suggests RNA might play important roles either structurally or catalytically in PB/SG. The paucity of only 79 other transcripts enriched is conceivably due to the complexity of the RNA mixture that is coisolated with Dhh1–GFP. It is estimated that 70% of cellular mRNA in yeast is associated with polyribosomes (Arava *et al.* 2003), and since ribosomal subunits are coisolated with Dhh1–GFP along with RNP complexes, the cellular mRNAs associated with ribosomal subunits can increase the overall background of RNA enrichment and decrease the effective enrichment of RNAs associated with RNP complexes. However, as the majority of RNA coisolating with Dhh1–GFP are noncoding, the identified transcripts are not isolated simply because of ribosome association.

We also show for the first time a physical association between PB and self-splicing introns within the mitochondrial *COX1* and 21S rRNA loci. Consistent with these findings, PB has been implicated in the splicing of mitochondrial introns as the respiratory deficiency of *dhh1Δ* and *lsm6Δ* mutants are rescued by deletion of the self-splicing mitochondrial introns (Luban *et al.* 2005). Another relevant aspect of self-splicing introns association with PB is their ability to act as mobile elements within the mitochondrial genome (Moran *et al.* 1992; Yang *et al.* 1996; Nielsen and Johansen 2009). PB components are required for retrotransposition of nuclear Ty elements that also localize to PB (Checkley *et al.* 2010). It is possible that PB play some role in regulating the mobility of self-splicing introns within the mitochondrial genome.

In conclusion, we have identified a class of proteins that controls PB formation, other classes that link PB assembly to other stress response protein foci, as well as several catalytic RNP complexes that connect PB with mitochondrial RNA processing. By isolating and determining the composition of PB in differential assembly conditions, we have identified components that would be undetectable by microscopy either because of low abundance, transient interactions, or association in nonstress conditions when foci are undetectable. These results demonstrate the usefulness of a global biochemical approach, complementary to cytological and genetic studies, which can enhance the understanding of RNP granule assembly and function.

ACKNOWLEDGMENTS

We thank Cecilia Garmendia-Torres for providing strains; John Aitchison for use of the planetary ball-mill grinder; Mark Gillespie for advice on antibody crosslinking; Gareth Cromie, Bruz Marzolf, and Pamela Troisch for advice on microarray analyses; Young-Ah Goo, David Goodlett, Deborah Chang, and Ryan Austin for advice on mass spectrometry analyses; Claire Gustafson for assistance in the early stages of the project; Cecilia Garmendia-Torres, David Morris, David Goodlett, John Aitchison, Dan Jarosz, and members of the Dudley lab for helpful discussions; and Cecilia Garmendia-Torres and John Woolford for helpful comments on the manuscript. Mass spectrometry was performed by Young-Ah Goo at the University of Washington School of Pharmacy’s Mass Spectrometry Facility. This work was supported by a strategic partnership between the Institute for Systems Biology and the University of Luxembourg, the National Institutes of Health (K22 HG002908, P50 GM076547 and N01-HV-28179), and Le Plan Technologies de la Santé par le Gouvernement du Grand-Duché de Luxembourg (to P.M.) through the Luxembourg Centre for Systems Biomedicine (LCSB), University of Luxembourg.

LITERATURE CITED

- Aizer, A., Y. Brody, L. W. Ler, N. Sonenberg, R. H. Singer *et al.*, 2008 The dynamics of mammalian P body transport, assembly, and disassembly in vivo. *Mol. Biol. Cell* 19: 4154–4166.
- Alberti, S., R. Halfmann, O. King, A. Kapila, and S. Lindquist, 2009 A systematic survey identifies prions and illuminates sequence features of prionogenic proteins. *Cell* 137: 146–158.
- Arava, Y., Y. Wang, J. D. Storey, C. L. Liu, P. O. Brown *et al.*, 2003 Genome-wide analysis of mRNA translation profiles in *Saccharomyces cerevisiae*. *Proc. Natl. Acad. Sci. USA* 100: 3889–3894.
- Arimoto, K., H. Fukuda, S. Imajoh-Ohmi, H. Saito, and M. Takekawa, 2008 Formation of stress granules inhibits apoptosis by suppressing stress-responsive MAPK pathways. *Nat. Cell Biol.* 10: 1324–1332.
- Bahassou-Benamri, R., A.-H. Davin, J.-C. Gaillard, B. Alonso, M. Odorico *et al.*, 2013 Subcellular localization and interaction network of the mRNA decay activator Pat1 upon UV stress. *Yeast* 30: 353–363.
- Balagopal, V., and R. Parker, 2009 Stm1 modulates mRNA decay and Dhh1 function in *Saccharomyces cerevisiae*. *Genetics* 181: 93–103.
- Benjamini, Y., and Y. Hochberg, 1995 Controlling the false discovery rate: a practical and powerful approach to multiple testing. *J.R. Stat. Soc.* 57: 289–300.
- Bonnerot, C., R. Boeck, and B. Lapeyre, 2000 The two proteins Pat1p (Mrt1p) and Spb8p interact in vivo, are required for mRNA decay, and are functionally linked to Pab1p. *Mol. Cell. Biol.* 20: 5939–5946.
- Borowski, L. S., R. J. Szczesny, L. K. Brzezniak, and P. P. Stepien, 2010 RNA turnover in human mitochondria: more questions than answers? *Biochim. Biophys. Acta* 1797: 1066–1070.
- Braisted, J. C., S. Kuntumalla, C. Vogel, E. M. Marcotte, A. R. Rodrigues *et al.*, 2008 The APEX Quantitative Proteomics Tool: generating protein quantitation estimates from LC-MS/MS proteomics results. *BMC Bioinformatics* 9: 529.

- Bregues, M., and R. Parker, 2007 Accumulation of polyadenylated mRNA, Pab1p, eIF4E, and eIF4G with P-bodies in *Saccharomyces cerevisiae*. *Mol. Biol. Cell* 18: 2592–2602.
- Bregues, M., D. Teixeira, and R. Parker, 2005 Movement of eukaryotic mRNAs between polysomes and cytoplasmic processing bodies. *Science* 310: 486–489.
- Bruni, F., P. Gramegna, R. N. Lightowers, and Z. M. A. Chrzanowska-Lightowers, 2012 The mystery of mitochondrial RNases. *Biochem. Soc. Trans.* 40: 865–869.
- Buchan, J. R., 2014 mRNP granules: assembly, function, and connections with disease. *RNA Biol.* 11: 1019–1030.
- Buchan, J. R., and R. Parker, 2009 Eukaryotic stress granules: the ins and outs of translation. *Mol. Cell* 36: 932–941.
- Buchan, J. R., D. Muhlrud, and R. Parker, 2008 P bodies promote stress granule assembly in *Saccharomyces cerevisiae*. *J. Cell Biol.* 183: 441–455.
- Buchan, J. R., T. Nissan, and R. Parker, 2010 Analyzing P-bodies and stress granules in *Saccharomyces cerevisiae*. *Methods Enzymol.* 470: 619–640.
- Buchan, J. R., J.-H. Yoon, and R. Parker, 2011 Stress-specific composition, assembly and kinetics of stress granules in *Saccharomyces cerevisiae*. *J. Cell Sci.* 124: 228–239.
- Buchan, J. R., R.-M. Kolaitis, J. P. Taylor, and R. Parker, 2013 Eukaryotic stress granules are cleared by autophagy and Cdc48/VCP function. *Cell* 153: 1461–1474.
- Castello, A., B. Fischer, K. Eichelbaum, R. Horos, B. M. Beckmann *et al.*, 2012 Insights into RNA biology from an atlas of mammalian mRNA-binding proteins. *Cell* 149: 1393–1406.
- Checkley, M. A., K. Nagashima, S. J. Lockett, K. M. Nyswaner, and D. J. Garfinkel, 2010 P-body components are required for Ty1 retrotransposition during assembly of retrotransposition-competent virus-like particles. *Mol. Cell Biol.* 30: 382–398.
- Cherkasov, V., S. Hofmann, S. Druffel-Augustin, A. Mogk, J. Tyedmers *et al.*, 2013 Coordination of translational control and protein homeostasis during severe heat stress. *Curr. Biol. CB* 23: 2452–2462.
- Coller, J. M., M. Tucker, U. Sheth, M. A. Valencia-Sanchez, and R. Parker, 2001 The DEAD box helicase, Dhh1p, functions in mRNA decapping and interacts with both the decapping and deadenylase complexes. *RNA* 7: 1717–1727.
- Costanzo, M. C., S. R. Engel, E. D. Wong, P. Lloyd, K. Karra *et al.*, 2014 *Saccharomyces* Genome Database provides new regulation data. *Nucleic Acids Res.* 42: D717–D725.
- Cougot, N., A. Cavalier, D. Thomas, and R. Gillet, 2012 The dual organization of P-bodies revealed by immunoelectron microscopy and electron tomography. *J. Mol. Biol.* 420: 17–28.
- Craig, R., and R. C. Beavis, 2004 TANDEM: matching proteins with tandem mass spectra. *Bioinformatics* 20: 1466–1467.
- Decker, C. J., and R. Parker, 2012 P-bodies and stress granules: possible roles in the control of translation and mRNA degradation. *Cold Spring Harb. Perspect. Biol.* 4: a012286.
- Decker, C. J., D. Teixeira, and R. Parker, 2007 Edc3p and a glutamine/asparagine-rich domain of Lsm4p function in processing body assembly in *Saccharomyces cerevisiae*. *J. Cell Biol.* 179: 437–449.
- Drummond, S. P., J. Hildyard, H. Firczuk, O. Reamtong, N. Li *et al.*, 2011 Diauxic shift-dependent relocalization of decapping activators Dhh1 and Pat1 to polysomal complexes. *Nucleic Acids Res.* 39: 7764–7774.
- Dunckley, T., M. Tucker, and R. Parker, 2001 Two related proteins, Edc1p and Edc2p, stimulate mRNA decapping in *Saccharomyces cerevisiae*. *Genetics* 157: 27–37.
- Dutrow, N., D. A. Nix, D. Holt, B. Milash, B. Dalley *et al.*, 2008 Dynamic transcriptome of *Schizosaccharomyces pombe* shown by RNA-DNA hybrid mapping. *Nat. Genet.* 40: 977–986.
- Escusa-Toret, S., W. I. M. Vonk, and J. Frydman, 2013 Spatial sequestration of misfolded proteins by a dynamic chaperone pathway enhances cellular fitness during stress. *Nat. Cell Biol.* 15: 1231–1243.
- Eulalio, A., I. Behm-Ansmant, and E. Izaurralde, 2007a P bodies: at the crossroads of post-transcriptional pathways. *Nat. Rev. Mol. Cell Biol.* 8: 9–22.
- Eulalio, A., I. Behm-Ansmant, D. Schweizer, and E. Izaurralde, 2007b P-body formation is a consequence, not the cause, of RNA-mediated gene silencing. *Mol. Cell Biol.* 27: 3970–3981.
- Fenger-Gron, M., C. Fillman, B. Norrild, and J. Lykke-Andersen, 2005 Multiple processing body factors and the ARE binding protein TTP activate mRNA decapping. *Mol. Cell* 20: 905–915.
- Garmendia-Torres, C., A. Skupin, S. A. Michael, P. Ruusuvoori, N. J. Kuwada *et al.*, 2014 Unidirectional P-body transport during the yeast cell cycle. *PLoS One* 9: e99428.
- Ghaemmaghami, S., W.-K. Huh, K. Bower, R. W. Howson, A. Belle *et al.*, 2003 Global analysis of protein expression in yeast. *Nature* 425: 737–741.
- Gilks, N., N. Kedersha, M. Ayodele, L. Shen, G. Stoecklin *et al.*, 2004 Stress granule assembly is mediated by prion-like aggregation of TIA-1. *Mol. Biol. Cell* 15: 5383–5398.
- Gingold, H., D. Tehler, N. R. Christoffersen, M. M. Nielsen, F. Asmar *et al.*, 2014 A dual program for translation regulation in cellular proliferation and differentiation. *Cell* 158: 1281–1292.
- Grousl, T., P. Ivanov, I. Frydlova, P. Vasicova, F. Janda *et al.*, 2009 Robust heat shock induces eIF2alpha-phosphorylation-independent assembly of stress granules containing eIF3 and 40S ribosomal subunits in budding yeast. *Saccharomyces cerevisiae*. *J. Cell Sci.* 122: 2078–2088.
- Grousl, T., P. Ivanov, I. Malcova, P. Pompach, I. Frydlova *et al.*, 2013 Heat shock-induced accumulation of translation elongation and termination factors precedes assembly of stress granules in *S. cerevisiae*. *PLoS One* 8: e57083.
- Han, D. K., J. Eng, H. Zhou, and R. Aebersold, 2001 Quantitative profiling of differentiation-induced microsomal proteins using isotope-coded affinity tags and mass spectrometry. *Nat. Biotechnol.* 19: 946–951.
- Han, T. W., M. Kato, S. Xie, L. C. Wu, H. Mirzaei *et al.*, 2012 Cell-free formation of RNA granules: bound RNAs identify features and components of cellular assemblies. *Cell* 149: 768–779.
- Harigaya, Y., B. N. Jones, D. Muhlrud, J. D. Gross, and R. Parker, 2010 Identification and analysis of the interaction between Edc3 and Dcp2 in *Saccharomyces cerevisiae*. *Mol. Cell Biol.* 30: 1446–1456.
- Hentze, M. W., and T. Preiss, 2010 The REM phase of gene regulation. *Trends Biochem. Sci.* 35: 423–426.
- Ho, C. H., L. Magtanong, S. L. Barker, D. Gresham, S. Nishimura *et al.*, 2009 A molecular barcoded yeast ORF library enables mode-of-action analysis of bioactive compounds. *Nat. Biotechnol.* 27: 369–377.
- Hogan, D. J., D. P. Riordan, A. P. Gerber, D. Herschlag, and P. O. Brown, 2008 Diverse RNA-binding proteins interact with functionally related sets of RNAs, suggesting an extensive regulatory system. *PLoS Biol.* 6: e255.
- Holcik, M., and N. Sonenberg, 2005 Translational control in stress and apoptosis. *Nat. Rev. Mol. Cell Biol.* 6: 318–327.
- Hoyle, N. P., L. M. Castelli, S. G. Campbell, L. E. A. Holmes, and M. P. Ashe, 2007 Stress-dependent relocalization of translationally primed mRNPs to cytoplasmic granules that are kinetically and spatially distinct from P-bodies. *J. Cell Biol.* 179: 65–74.
- Hu, W., T. J. Sweet, S. Chamnongpol, K. E. Baker, and J. Coller, 2009 Co-translational mRNA decay in *Saccharomyces cerevisiae*. *Nature* 461: 225–229.
- Hu, Z., A. Zhang, G. Storz, S. Gottesman, and S. H. Leppla, 2006 An antibody-based microarray assay for small RNA detection. *Nucleic Acids Res.* 34: e52.
- Huang, H.-R., C. E. Rowe, S. Mohr, Y. Jiang, A. M. Lambowitz *et al.*, 2005 The splicing of yeast mitochondrial group I and group II introns requires a. *Proc. Natl. Acad. Sci. USA* 102: 163–168.
- Huh, W.-K., J. V. Falvo, L. C. Gerke, A. S. Carroll, R. W. Howson *et al.*, 2003 Global analysis of protein localization in budding yeast. *Nature* 425: 686–691.
- Hurto, R. L., and A. K. Hopper, 2011 P-body components, Dhh1 and Pat1, are involved in tRNA nuclear-cytoplasmic dynamics. *RNA* 17: 912–924.
- Kato, M., T. W. Han, S. Xie, K. Shi, X. Du *et al.*, 2012 Cell-free formation of RNA granules: low complexity sequence domains form dynamic fibers within hydrogels. *Cell* 149: 753–767.

- Kedersha, N., and P. Anderson, 2009 Regulation of translation by stress granules and processing bodies. *Prog. Mol. Biol. Transl. Sci.* 90: 155–185.
- Kedersha, N., G. Stoeklin, M. Ayodele, P. Yacono, J. Lykke-Andersen *et al.*, 2005 Stress granules and processing bodies are dynamically linked sites of mRNP remodeling. *J. Cell Biol.* 169: 871–884.
- Kedersha, N., P. Ivanov, and P. Anderson, 2013 Stress granules and cell signaling: more than just a passing phase? *Trends Biochem. Sci.* 38: 494–506.
- Keller, A., A. I. Nesvizhskii, E. Kolker, and R. Aebersold, 2002 Empirical statistical model to estimate the accuracy of peptide identifications made by MS/MS and database search. *Anal. Chem.* 74: 5383–5392.
- Kressler, D., J. de la Cruz, M. Rojo, and P. Linder, 1997 Fall1p is an essential DEAD-box protein involved in 40S-ribosomal-subunit biogenesis in *Saccharomyces cerevisiae*. *Mol. Cell Biol.* 17: 7283–7294.
- Kshirsagar, M., and R. Parker, 2004 Identification of Edc3p as an enhancer of mRNA decapping in *Saccharomyces cerevisiae*. *Genetics* 166: 729–739.
- Lardenois, A., Y. Liu, T. Walther, F. Chalmel, B. Evrard *et al.*, 2011 Execution of the meiotic noncoding RNA expression program and the onset of gametogenesis in yeast require the conserved exosome subunit Rrp6. *Proc. Natl. Acad. Sci. USA* 108: 1058–1063.
- Lavut, A., and D. Raveh, 2012 Sequestration of highly expressed mRNAs in cytoplasmic granules, P-bodies, and stress granules enhances cell viability. *PLoS Genet.* 8: e1002527.
- Lee, S.-I., A. M. Dudley, D. Drubin, P. A. Silver, N. J. Krogan *et al.*, 2009 Learning a prior on regulatory potential from eQTL data. *PLoS Genet.* 5: e1000358.
- Li, Y. R., O. D. King, J. Shorter, and A. D. Gitler, 2013 Stress granules as crucibles of ALS pathogenesis. *J. Cell Biol.* 201: 361–372.
- Luban, C., M. Beutel, U. Stahl, and U. Schmidt, 2005 Systematic screening of nuclear encoded proteins involved in the splicing metabolism of group II introns in yeast mitochondria. *Gene* 354: 72–79.
- Lui, J., S. G. Campbell, and M. P. Ashe, 2010 Inhibition of translation initiation following glucose depletion in yeast facilitates a rationalization of mRNA content. *Biochem. Soc. Trans.* 38: 1131–1136.
- Marnef, A., and N. Standart, 2010 Pat1 proteins: a life in translation, translation repression and mRNA decay. *Biochem. Soc. Trans.* 38: 1602–1607.
- Matsumoto, K., M. Minami, F. Shinozaki, Y. Suzuki, K. Abe *et al.*, 2011 Hsp90 is involved in the formation of P-bodies and stress granules. *Biochem. Biophys. Res. Commun.* 407: 720–724.
- Mellacheruvu, D., Z. Wright, A. L. Couzens, J.-P. Lambert, N. A. St-Denis *et al.*, 2013 The CRAPome: a contaminant repository for affinity purification-mass spectrometry data. *Nat. Methods* 10: 730–736.
- Mitchell, S. F., S. Jain, M. She, and R. Parker, 2013 Global analysis of yeast mRNPs. *Nat. Struct. Mol. Biol.* 20: 127–133.
- Moran, J. V., C. M. Wernette, K. L. Mecklenburg, R. A. Butow, and P. S. Perlman, 1992 Intron 5 alpha of the COXI gene of yeast mitochondrial DNA is a mobile group I intron. *Nucleic Acids Res.* 20: 4069–4076.
- Nadler-Holly, M., M. Breker, R. Gruber, A. Azia, M. Gymrek *et al.*, 2012 Interactions of subunit CCT3 in the yeast chaperonin CCT/TRiC with Q/N-rich proteins revealed by high-throughput microscopy analysis. *Proc. Natl. Acad. Sci. USA* 109: 18833–18838.
- Narayanaswamy, R., M. Levy, M. Tsechansky, G. M. Stovall, J. D. O'Connell *et al.*, 2009 Widespread reorganization of metabolic enzymes into reversible assemblies upon nutrient starvation. *Proc. Natl. Acad. Sci. USA* 106: 10147–10152.
- Nesvizhskii, A. I., A. Keller, E. Kolker, and R. Aebersold, 2003 A statistical model for identifying proteins by tandem mass spectrometry. *Anal. Chem.* 75: 4646–4658.
- Nielsen, H., and S. D. Johansen, 2009 Group I introns: moving in new directions. *RNA Biol.* 6: 375–383.
- Novotny, I., K. Podolska, M. Blazikova, L. S. Valasek, P. Svoboda *et al.*, 2012 Nuclear LSm8 affects number of cytoplasmic processing bodies via controlling cellular distribution of Like-Sm proteins. *Mol. Biol. Cell* 23: 3776–3785.
- O'Connell, J. D., A. Zhao, A. D. Ellington, and E. M. Marcotte, 2012 Dynamic reorganization of metabolic enzymes into intracellular bodies. *Annu. Rev. Cell Dev. Biol.* 28: 89–111.
- O'Connell, J. D., M. Tsechansky, A. Royall, D. R. Boutz, A. D. Ellington *et al.*, 2014 A proteomic survey of widespread protein aggregation in yeast. *Mol. Biosyst.* 10: 851–861.
- Oeffinger, M., K. E. Wei, R. Rogers, J. A. DeGrasse, B. T. Chait *et al.*, 2007 Comprehensive analysis of diverse ribonucleoprotein complexes. *Nat. Methods* 4: 951–956.
- Pullmann, R. J., H. H. Kim, K. Abdelmohsen, A. Lal, J. L. Martindale *et al.*, 2007 Analysis of turnover and translation regulatory RNA-binding protein expression through binding to cognate mRNAs. *Mol. Cell Biol.* 27: 6265–6278.
- Ramachandran, V., K. H. Shah, and P. K. Herman, 2011 The cAMP-dependent protein kinase signaling pathway is a key regulator of P body foci formation. *Mol. Cell* 43: 973–981.
- Ramaswami, M., J. P. Taylor, and R. Parker, 2013 Altered ribostasis: RNA-protein granules in degenerative disorders. *Cell* 154: 727–736.
- Reijns, M. A. M., R. D. Alexander, M. P. Spiller, and J. D. Beggs, 2008 A role for Q/N-rich aggregation-prone regions in P-body localization. *J. Cell Sci.* 121: 2463–2472.
- Rikhvanov, E. G., N. V. Romanova, and Y. O. Chernoff, 2007 Chaperone effects on prion and nonprion aggregates. *Prion* 1: 217–222.
- Rinnerthaler, M., R. Lejskova, T. Grousl, V. Stradalova, G. Heeren *et al.*, 2013 Mmi1, the yeast homologue of mammalian TCTP, associates with stress granules in heat-shocked cells and modulates proteasome activity. *PLoS One* 8: e77791.
- Rose, M. D., F. M. Winston, and P. Hieter, 1990 *Methods in Yeast Genetics: A Laboratory Course Manual*. Cold Spring Harbor Laboratory Press, Cold Spring Harbor, NY.
- Scherrer, T., N. Mittal, S. C. Janga, and A. P. Gerber, 2010 A screen for RNA-binding proteins in yeast indicates dual functions for many enzymes. *PLoS One* 5: e15499.
- Segal, S. P., T. Dunkley, and R. Parker, 2006 Sbp1p affects translational repression and decapping in *Saccharomyces cerevisiae*. *Mol. Cell Biol.* 26: 5120–5130.
- Shah, K. H., R. Nostramo, B. Zhang, S. N. Varia, B. M. Klett *et al.*, 2014 Protein kinases are associated with multiple, distinct cytoplasmic granules in quiescent yeast cells. *Genetics* 198: 1495–1512.
- Sheth, U., and R. Parker, 2003 Decapping and decay of messenger RNA occur in cytoplasmic processing bodies. *Science* 300: 805–808.
- Sheth, U., and R. Parker, 2006 Targeting of aberrant mRNAs to cytoplasmic processing bodies. *Cell* 125: 1095–1109.
- Simpson, C. E., and M. P. Ashe, 2012 Adaptation to stress in yeast: to translate or not? *Biochem. Soc. Trans.* 40: 794–799.
- Smith-Kinnaman, W. R., M. J. Berna, G. O. Hunter, J. D. True, P. Hsu *et al.*, 2014 The interactome of the atypical phosphatase Rtr1 in *Saccharomyces cerevisiae*. *Mol. Biosyst.* 10: 1730–1741.
- Smyth, G., 2005 Limma: linear models for microarray data, pp. 397–420 in *Bioinformatics and Computational Biology Solutions using R and Bioconductor*, edited by Gentleman, R., V. Carey, S. Dudoit, R. Irizarry, and W. Huber. Springer, New York.
- Solem, A., N. Zingler, and A. M. Pyle, 2006 A DEAD protein that activates intron self-splicing without unwinding RNA. *Mol. Cell* 24: 611–617.
- Sontag, E. M., W. I. M. Vonk, and J. Frydman, 2014 Sorting out the trash: the spatial nature of eukaryotic protein quality control. *Curr. Opin. Cell Biol.* 26: 139–146.
- Stoeklin, G., and N. Kedersha, 2013 Relationship of GW/P-bodies with stress granules. *Adv. Exp. Med. Biol.* 768: 197–211.
- Stribinski, V., and K. S. Ramos, 2007 Rpm2p, a protein subunit of mitochondrial RNase P, physically and genetically interacts with cytoplasmic processing bodies. *Nucleic Acids Res.* 35: 1301–1311.
- Subramaniam, A. R., B. M. Zid, and E. K. O'Shea, 2014 An integrated approach reveals regulatory controls on bacterial translation elongation. *Cell* 159: 1200–1211.
- Sulo, P., K. R. Groom, C. Wise, M. Steffen, and N. Martin, 1995 Successful transformation of yeast mitochondria with RPM1: an approach for in vivo studies of mitochondrial RNase P RNA structure, function and biosynthesis. *Nucleic Acids Res.* 23: 856–860.

- Summers, D. W., P. M. Douglas, and D. M. Cyr, 2009 Prion propagation by Hsp40 molecular chaperones. *Prion* 3: 59–64.
- Sweet, T., C. Kovalak, and J. Collier, 2012 The DEAD-box protein Dhh1 promotes decapping by slowing ribosome movement. *PLoS Biol.* 10: e1001342.
- Swisher, K. D., and R. Parker, 2010 Localization to, and effects of Pbp1, Pbp4, Lsm12, Dhh1, and Pab1 on stress granules in *Saccharomyces cerevisiae*. *PLoS One* 5: e10006.
- Szczesny, R. J., M. A. Wojcik, L. S. Borowski, M. J. Szewczyk, M. M. Skrok *et al.*, 2013 Yeast and human mitochondrial helicases. *Biochim. Biophys. Acta* 1829: 842–853.
- Tackett, A. J., J. A. DeGrasse, M. D. Sekedat, M. Oeffinger, M. P. Rout *et al.*, 2005 I-DIRT, a general method for distinguishing between specific and nonspecific protein interactions. *J. Proteome Res.* 4: 1752–1756.
- Teixeira, D., and R. Parker, 2007 Analysis of P-body assembly in *Saccharomyces cerevisiae*. *Mol. Biol. Cell* 18: 2274–2287.
- Teixeira, D., U. Sheth, M. A. Valencia-Sanchez, M. Brengues, and R. Parker, 2005 Processing bodies require RNA for assembly and contain non-translating mRNAs. *RNA* 11: 371–382.
- Tharun, S., W. He, A. E. Mayes, P. Lennertz, J. D. Beggs *et al.*, 2000 Yeast Sm-like proteins function in mRNA decapping and decay. *Nature* 404: 515–518.
- Tian, Y., Y. Zhou, S. Elliott, R. Aebersold, and H. Zhang, 2007 Solid-phase extraction of N-linked glycopeptides. *Nat. Protoc.* 2: 334–339.
- Tkach, J. M., A. Yimit, A. Y. Lee, M. Riffle, M. Costanzo *et al.*, 2012 Dissecting DNA damage response pathways by analysing protein localization and abundance changes during DNA replication stress. *Nat. Cell Biol.* 14: 966–976.
- Tsvetanova, N. G., D. M. Klass, J. Salzman, and P. O. Brown, 2010 Proteome-wide search reveals unexpected RNA-binding proteins in *Saccharomyces cerevisiae*. *PLoS One* 5: e12671.
- Vogel, C., and E. M. Marcotte, 2008 Calculating absolute and relative protein abundance from mass spectrometry-based protein expression data. *Nat. Protoc.* 3: 1444–1451.
- Walters, R. W., D. Muhlrad, J. Garcia, and R. Parker, 2015 Differential effects of Ydj1 and Sis1 on Hsp70-mediated clearance of stress granules in *Saccharomyces cerevisiae*. *RNA* 21: 1660–1671.
- Weidner, J., C. Wang, C. Prescianotto-Baschong, A. F. Estrada, and A. Spang, 2014 The polysome-associated proteins Scp160 and Bfr1 prevent P body formation under normal growth conditions. *J. Cell Sci.* 127: 1992–2004.
- Wildburger, N. C., S. R. Ali, W.-C. J. Hsu, A. S. Shavkunov, M. N. Nenov *et al.*, 2015 Quantitative proteomics reveals protein-protein interactions with fibroblast growth factor 12 as a component of the voltage-gated sodium channel 1.2 (nav1.2) macromolecular complex in Mammalian brain. *Mol. Cell. Proteomics MCP* 14: 1288–1300.
- Winston, F., C. Dollard, and S. L. Ricupero-Hovasse, 1995 Construction of a set of convenient *Saccharomyces cerevisiae* strains that are isogenic to S288C. *Yeast* 11: 53–55.
- Wootton, J. C., 1994 Non-globular domains in protein sequences: automated segmentation using complexity measures. *Comput. Chem.* 18: 269–285.
- Xu, Z., W. Wei, J. Gagneur, F. Perocchi, S. Clauder-Munster *et al.*, 2009 Bidirectional promoters generate pervasive transcription in yeast. *Nature* 457: 1033–1037.
- Yang, J., S. Zimmerly, P. S. Perlman, and A. M. Lambowitz, 1996 Efficient integration of an intron RNA into double-stranded DNA by reverse splicing. *Nature* 381: 332–335.
- Yang, X., Y. Shen, E. Garre, X. Hao, D. Krumlinde *et al.*, 2014 Stress granule-defective mutants deregulate stress responsive transcripts. *PLoS Genet.* 10: e1004763.

Communicating editor: D. J. Gresham